JOURNAL OF PETROLOGY | VOLUME 38 | NUMBER 6 | PAGES 703–725 | 1997

Platinum Group Element Segregation and Mineralization in a Noritic Ring Complex Formed from Proterozoic Siliceous High Magnesium Basalt Magmas in the Vestfold Hills, Antarctica

H.-MICHAEL SEITZ[1]* AND REID R. KEAYS[2]

[1]GEOLOGY DEPARTMENT, UNIVERSITY OF TASMANIA, HOBART, TAS. 7001, AUSTRALIA

[2]MINERAL EXPLORATION RESEARCH CENTRE, LAURENTIAN UNIVERSITY, SUDBURY, ONT., CANADA P3E 2C6

RECEIVED MAY 2, 1996 REVISED TYPESCRIPT ACCEPTED JANUARY 10, 1997

Siliceous High Magnesium Basalt (SHMB) magmas have been implied to play critical roles in the formation of platiniferous horizons in layered intrusions such as the Bushveld Complex, South Africa. However, their role in the formation of such complexes and particularly in the generation of the Cu–Ni–Platinum Group Element (PGE) sulphide mineralization has been deduced rather than proven. In this paper, we present an example of Cu–Ni–PGE sulphide mineralization which was unequivocally formed from SHMB magmas. This example is provided by the Noritic Ring Complex of the northern Vestfold Hills of Antarctica. The Noritic Ring Complex is co-magmatic with the early Proterozoic High Magnesium Tholeiite (HMT) dykes which were previously demonstrated to have formed from SHMB magmas. Chilled margins from the HMT have very similar PGE (average values: 16·0 p.p.b. Pd, 15·2 p.p.b. Pt, 0·98 p.p.b. Ru, 0·34 p.p.b. Ir) and other chemical features common to SHMB volcanics and intrusives from Western Australia, as well as to sills from the Bushveld Complex that are believed to have formed from the magmas that formed the Critical Zone of the Complex. The high Pd and Pt contents combined with the low S contents (291 p.p.m.) of the HMT dykes indicate that they were formed from S-undersaturated magmas, a fundamental requirement for the formation of major Cu–Ni–PGE sulphide mineralization. Sub-economic Cu–Ni–PGE sulphide mineralization occurs as disseminated sulphides and sulphide lenses within the last intrusive phase of the Noritic Ring Complex, the Rubbly Norite, which is characterized by the presence of up to 40 modal % orthopyroxene phenocrysts as well as xenoliths of country rock. It is suggested that the SHMB magma which formed the Rubbly Norite lagged behind the rest of the SHMB magma and spent some time in a residence chamber below the Noritic Ring Complex in which it underwent cooling, assimilation of country rock fragments and extensive crystallization of orthopyroxene which accumulated along the floor of the temporary magma chamber. These factors caused S saturation of the SHMB magma and the generation of the Cu–Ni–PGE sulphides which accumulated along with the orthopyroxene phenocrysts; the orthopyroxene- and sulphide-bearing magma was subsequently emplaced into the Noritic Ring Complex magma chamber. Economic concentrations of Cu–Ni–PGE sulphides did not form in the Noritic Ring Complex because the SHMB magmas did not interact with an abundant source of S.

KEY WORDS: *Platinum Group Elements; Siliceous High Magnesium Basalts; Vestfold Hills—Antarctica*

INTRODUCTION

Siliceous High Magnesium Basalt (SHMB) magmas are believed to play a fundamental role in the generation of Platinum Group Element (PGE) mineralization in layered intrusions such as the Bushveld Complex (Sun *et al.*,

*Corresponding author. Present address: Mineralogisches Institut, Universität Heidelberg, Im Neuenheimer Feld 236, 69120 Heidelberg, Germany. Telephone: 00 49-6221-54 6038. Fax: 00 49-6221-54 4805. e-mail: mseitz@classic.min.uni-heidelberg.de

1989, 1991). This feature arises because they are a member of a select group of magmas that were S undersaturated at the time of magma generation and emplacement; as shown by Keays (1995), S-undersaturated magmas are the only magma types that are capable of forming major Cu–Ni–PGE sulphide deposits. Owing to the extremely high partition coefficients of the PGE between sulphide melt and silicate melt (e.g. Peach *et al.*, 1994), S-saturated magmas have very low PGE contents, which were retained within residual magmatic sulphides in the source region.

Although SHMB may play a critical role in the formation of Cu–Ni–PGE mineralization in layered intrusions and possibly also in the generation of Archaean Au deposits (see Keays, 1983, 1987), they are a relatively newly 'recognized' rock type that has thus far only been described from a few localities. They are known to occur in Archaean greenstone belts where they are associated with komatiites and Cu–Ni–PGE mineralization (Redman & Keays, 1985). In addition, they are believed to have been the parental magmas which formed the ultramafic portions of layered intrusions in the Pilbara Archaean craton of Western Australia (Sun *et al.*, 1991); as shown by Hoatson & Keays (1989), some of these, such as the Munni Munni Intrusion, contain significant PGE mineralization. Another example of rocks formed by SHMB is the Scourie Dykes (Sun *et al.*, 1989).

The genesis of SHMB has been a matter of debate. Whereas Redman & Keays (1985) concluded that the SHMB in the Kambalda area of Western Australia were the Archaean analogues of modern boninites, both Arndt & Jenner (1986) and Sun *et al.* (1989) argued that they were the products of assimilation–fractional crystallization (AFC) processes involving the assimilation of large volumes of crustal material. Similarly, whereas Hamlyn & Keays (1986) and Hatton & Sharpe (1989) argued that the parental magmas (and hence, the magmas responsible for the PGE mineralization of the Merensky Reef) to the Critical Zone of the Bushveld Complex were boninites, Sun *et al.* (1989) concluded that they were SHMB that had formed by AFC processes involving the assimilation of ~14% felsic crust and 35% crystal fractionation.

Proterozoic-aged SHMB occur as dykes in both the Vestfold Hills and the Napier Complex of Antarctica. To avoid any genetic interpretations, Kuehner (1989) described the Vestfold Hills dykes as High Magnesium Tholeiites (HMT), a term that is retained in this paper. Kuehner (1989) showed that they were similar in composition to not only modern-day boninites but also micropyroxenite sills from the Bushveld Complex, which Sharpe & Hulbert (1985) had concluded had been formed from remobilized suspensions of Lower Zone cumulates in a parental magma with boninite affinities. Kuehner (1989) concluded that the Vestfold Hills HMT were also 'boninite-like' and concluded that their parental magmas had to have been formed at low pressures (7–8 kbar) and shallow depths (25–28 km). In the same volume, Sun *et al.* (1989) argued that they had been formed from crustally contaminated komatiites.

In this study, we have carried out PGE analyses not only on samples from the HMT (SHMB) dykes but also on Cu–Ni–PGE sulphide-bearing samples from a comagmatic Noritic Ring Complex (NRC) of the Vestfold Hills. (The term ring complex is used here in a descriptive manner, with no genetic connotation.) In this contribution, we will describe the Cu–Ni–PGE sulphide mineralization, attempt to evaluate its mode of formation, and finally discuss the petrogenesis of the parental magmas to both the HMT dykes as well as the NRC. This study has afforded another opportunity to evaluate the two petrogenetic models for the origin of SHMB, namely, crustal contamination of komatiites or relatively shallow melting of an enriched mantle source region akin to the generation of boninites.

REGIONAL GEOLOGY

The East Antarctic Shield, which has been a relatively stable craton for the last 2·5–3·0 Ga, comprises mainly Archaean and Proterozoic terranes (James & Tingey, 1983). Outcrops along the East Antarctic coast occur in the Vestfold Hills, Bunger Hills and the Prince Charles Mountains (Fig. 1a), and furthermore in Commonwealth Bay and the Napier Complex of Enderby Land. During early to middle Proterozoic time, over a period of ~1·3 Ga, mafic dyke swarms were intruded in distinct magmatic episodes and of various compositions into both Archaean and Proterozoic crust of the Vestfold Block (Fig. 1c).

The Vestfold Hills have had a complex late Archaean and Proterozoic deformational and thermal history (Oliver *et al.*, 1982; Parker *et al.*, 1983; Kuehner & Green, 1987; Passchier *et al.*, 1990; Hoek & Passchier, 1991; Seitz, 1994; Dirks *et al.*, 1994; Hoek & Seitz, 1995). Two major high-grade metamorphic events have been recognized in the Vestfold Block. The first, granulite facies event took place between 3·0 and 2·4 Ga under peak P–T conditions of 700–1000°C and 8–10 kbar (Collerson *et al.*, 1983). The second metamorphic event, which reached amphibolite to granulite facies conditions in the Vestfold Hills, occurred after the emplacement of the youngest dyke suite, at ~1025 Ma (Black *et al.*, 1991) and at P–T conditions of 600–800°C and 6–8 kbar. The more recent studies of Passchier *et al.* (1990) show that the currently exposed part of the Vestfold Hills was uplifted to shallow crustal levels before the emplacement of the youngest dyke suite. The observed pseudotachylites predating the youngest dyke suites (~1250 Ma) indicate

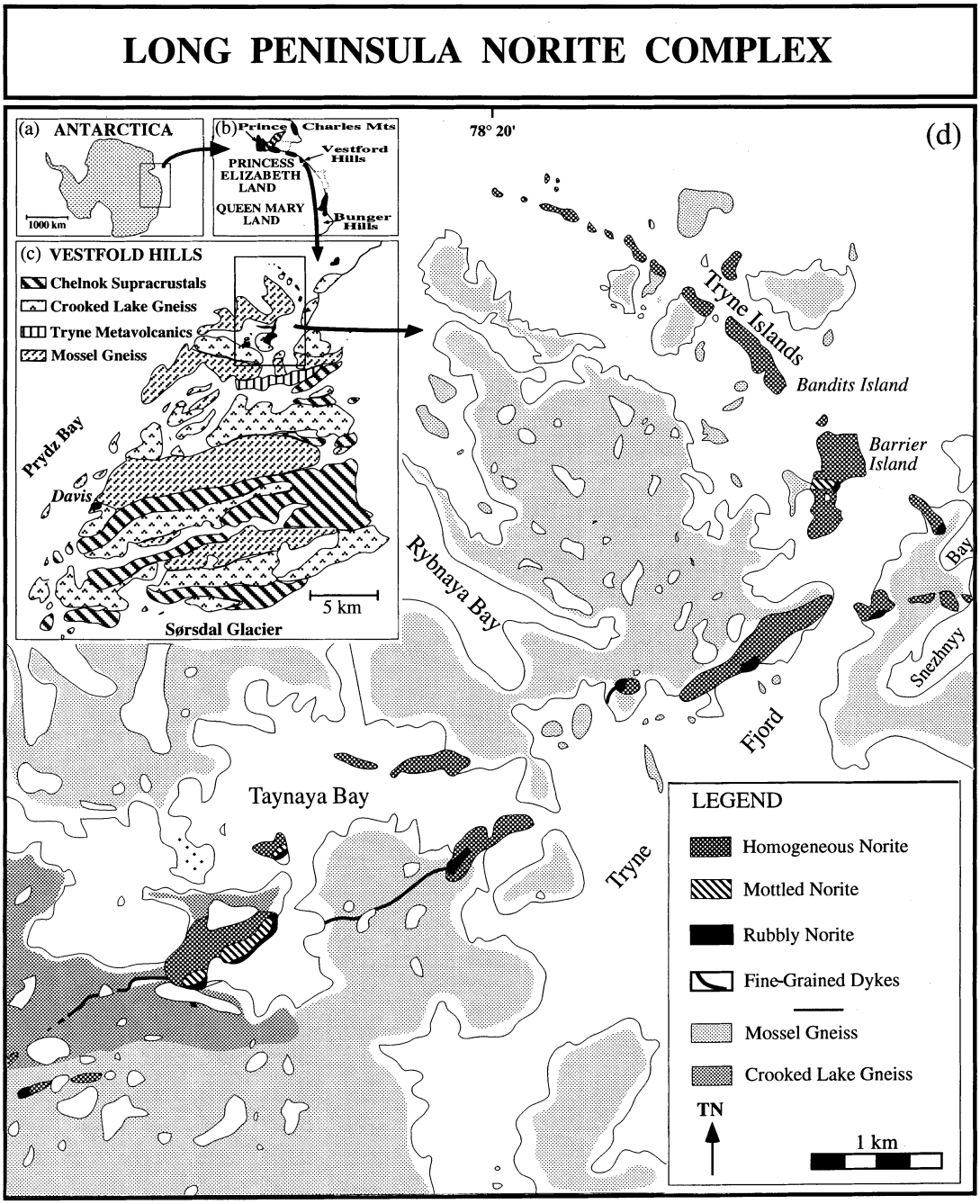

Fig. 1. Maps of East Antarctica showing locations of metamorphic complexes of the Prince Charles Mountains, Bunger Hills and the Vestfold Hills (b and c). The Noritic Ring Complex of the northern Vestfold Hills (Long Peninsula) is shown in detail (d).

brittle faulting in the uppermost levels of the crust at probably ~3 kbar.

The dyke suites were emplaced during three major magmatic episodes (Table 1). The first episode is dominated by olivine tholeiites (HMT) occurring throughout the Vestfold Hills and in the Napier Complex. Rb–Sr whole-rock isochrons yield ages of 2424±72 Ma for Group I HMT (Sheraton & Black, 1981; Collerson & Sheraton, 1986). Some Fe-rich tholeiite (FRT) dykes were contemporaneously emplaced with these HMT dykes (Kuehner, 1987). U–Pb zircon dating (Lanyon *et al.*, 1993) gives ages of 2241±4 Ma for the younger of the two main HMT dyke suites to which the norite belongs. Lanyon *et al.* (1993) obtained ages of 2241±4

Table 1: Classification scheme for the mafic dykes of the Vestfold Hills

Dyke suite	Group	Major magmatic episode	Time (Ma)	Dating method
High-Mg Tholeiite dykes	HMT group I, Ia	1	2424–2350	Rb–Sr
Fe-rich Tholeiite dykes	FRT HiTi group	1		
High-Mg Tholeiite dykes	HMT group II, IIa, III	1	2241	U–Pb
Fe-rich Tholeiite dykes	FRT LoTi group, PM group	1		
Fe-rich Tholeiite dykes	FRT	2	1754	U–Pb
Lamprophyre dykes		3		
Fe-rich Tholeiite dykes	FRT sub-groups 1–9	3	1380	U–Pb
Lamprophyre dykes		3		
Fe-rich Tholeiite dykes	FRT sub-groups 1–9	3	248	U–Pb

Classification of the HMT after Seitz (1991) and FRT after Kuehner (1986, 1987).

Ma and 2238 ± 7 Ma for the Homogeneous Norite and Mottled Norite, respectively (Table 1). The HMT and the norite were emplaced into shallow crustal levels. Pressure and temperature of emplacement for Group I HMT were estimated to be ~1250°C at 1–5 kbar (Seitz, 1994). The *P–T* estimates for Group II and IIa HMT (including the norite) indicate temperatures of 1200–1250°C and pressures between 2 and 4·5 kbar (Seitz, 1991). These results are in accordance with pressure estimates (3–4 kbar) derived independently from sapphirine-bearing xenoliths occurring within the norite (Harley & Christy, 1995).

During the second magmatic episode a small suite of FRT dykes were intruded, giving an Rb–Sr whole-rock isochron age of 1791 ± 62 Ma (Sheraton & Collerson, 1983). U–Pb zircon ages indicate emplacement of these dykes at ~1754 ± 16 Ma (Lanyon *et al.*, 1993).

Abundant dykes were emplaced during the final magmatic episode. The FRT belonging to this suite were described by Collerson & Sheraton (1986) and yield an Rb–Sr whole-rock isochron age of 1374 ± 125 Ma. U–Pb data yield ages of 1380 ± 7 Ma for one suite of dykes and 1241 ± 5 Ma for a second suite (Lanyon *et al.*, 1993). Lamprophyric dykes were emplaced during the same magmatic episode; although relatively widespread, they are voluminously subordinate. Crosscutting relationships between lamprophyre and tholeiite dykes clearly show that the former were emplaced during both the 1380 Ma and 1241 Ma magmatic episodes (Seitz, 1991; Hoek & Seitz, 1995).

The NRC of the Northern Vestfold Hills is a large intrusive dyke that occurs in the Long Peninsula area (Fig. 1d). This semicircular complex has a diameter of ~7–8 km and comprises several discrete bodies which vary in width from 70 to 400 m. Outcrops occur to the southwest of Taynaya Bay, on the western shore of Tryne Fjord and on the western part of Snezhnyy Bay, and can be traced along the Tryne Islands (e.g. Barrier and Bandits Island, Fig. 1d). Bodies in the north, on the Tryne Islands, become progressively narrower in width westwards. The more voluminous southern branch continues through the western part of Long Peninsula, occurring in smaller pods along the southwestern extension of Taynaya Bay area and in elongated bodies extending to the western part of Long Fjord (~1 km SE of Ace Lake). Fine-grained dykes which were emplaced contemporaneously with the NRC link several discrete norite bodies. The NRC was emplaced during early Proterozoic time and has intruded various Archaean orthogneiss units. Contacts between the NRC and the country rock are often sharp, with the complex exhibiting chilled margins. Occasionally, 1–2 m wide schlieren structures occur within the country rocks at the complex margins, reflecting partial melting and assimilation of wall-rock. The margins of the ring complex dip steeply, between 60° and 90°, and may be inclined inwards or outwards.

The NRC was first reported by McLeod & Harding (1967), and was described in more detail by Kuehner (1986). Seitz (1991) recognized three distinct lithological units:

(1) The Homogeneous Norite, the most voluminous unit (70–80%), is composed of orthopyroxene, clinopyroxene and plagioclase; orthopyroxene-phyric fine-grained dykes appear to be related to the Homogeneous Norite;

(2) the Mottled Norite, a unit characterized by large (1–2 cm) plagioclase–alkali-feldspar aggregates;

(3) the Rubbly Norite, a less common variant (~10%), which is distinguished by patches of bronzitic orthopyroxene, cognate and inherited xenoliths, and globules of sulphide.

Contact relationships between the Rubbly Norite and the Homogeneous Norite suggest multiple intrusion within the complex. The borders between these norite types are always steeply dipping, and field as well as microscopic observations suggest a sequence of emplacement in which the Rubbly Norite was the later body to be emplaced. The features which make the Mottled Norite distinguishable from the Homogeneous Norite are interpreted as *in situ* differentiation processes following emplacement. Whereas sharp contacts are observed between the Rubbly Norite and both the Mottled Norite and Homogeneous Norite, borders between the Homogeneous and Mottled Norite are always gradational, suggesting contemporaneous emplacement.

The NRC is believed to be a member of the HMT dyke suite of the Vestfold Hills. The NRC post-dates the first dyke set of the HMT but predates subsequent dyke suites. Several HMT dykes may be traced into the complex (Fig. 1d). It remains uncertain, however, whether these dykes are feeders or products of the complex. The HMT dyke suite has been subdivided into three main groups and two sub-groups according to crosscutting relationships, petrography and geochemistry (Kuehner, 1987; Seitz, 1991, 1994; Hoek & Seitz, 1995).

Xenoliths occurring in the Rubbly Norite are mostly orthopyroxenites but also include websterite, sapphirine-bearing fine-grained quartzite and feldspathic gneiss. Cognate enstatite nodules are common too. Sulphide-rich zones occur in most outcrops of the Rubbly Norite and vary in size from 4 to 6 m, up to 30 m in width and extending up to 400 m in length. The largest of these sulphide-bearing bodies occur in the southern part of the complex. As will be shown, the sulphide-bearing zones carry significant PGE. Dispersed sulphide (and oxide) phases are also present in the other norite units (i.e. the Homogeneous Norite and the Mottled Norite) but are more abundant in the Rubbly Norite.

ANALYTICAL METHODS

Twenty-seven samples from the Homogeneous and Mottled Norites, the Rubbly Norite, the chilled margins of fine-grained dykes associated with the norite, and from chilled margins of other HMT dykes from the Vestfold Hills were analysed for PGE, S, Ni, Cu and Zn (Table 2).

The PGE and Au were analysed at the University of Melbourne (Australia) and by two commercial laboratories [Analytical Services (W.A.) Pty Ltd and Nuclear Activation Services Ltd, Ont., Canada]. All laboratories preconcentrated PGEs and Au by fire assay. The analytical techniques employed by the various laboratories were radiochemical neutron activation analysis (RNAA), inductively coupled plasma-mass spectrometry (ICP-MS) and instrumental neutron activation analysis (INAA), respectively. The RNAA method, using NiS fire assay preconcentration, has been described by Hoatson & Keays (1989). Detection limits for various elements are typically 0·01–0·2 p.p.b. for Au and Ir, and 0·2–0·5 p.p.b. for Pt, Pd and Ru.

Sulphur was analysed in 16 samples by LECO iodate titration, and Ni, Cu and Zn by X-ray fluorescence (XRF; Table 2). Major and trace element analyses (Table 3) were determined by XRF spectrometry using an automated Philips PW 1410 spectrometer. Rare earth elements (REE) were determined by the ion-exchange technique after Robinson *et al.* (1986). A CAMECA SX 50 electron microprobe fitted with a wavelength-dispersive analytical system was also used, operating at a beam current of 20 nA and accelerating voltage of 15 kV for silicates, and 100 nA and 20 kV for sulphides and PGE minerals (Table 4).

PETROGRAPHY AND MINERAL CHEMISTRY

Homogeneous Norite

Macroscopically, the Homogeneous Norite appears as a uniform, medium- to coarse-grained rock. The mineral assemblages comprise orthopyroxene with minor clinopyroxene and plagioclase of cumulate texture. The orthopyroxenes are bronzites of up to 7 mm in length. After the classification of Wager *et al.* (1960), they represent orthopyroxene orthocumulates.

Orthopyroxenes are often rimmed by pigeonite (now inverted), with intercumulus phases consisting mainly of dusty plagioclase and clinopyroxene. The interstices between clinopyroxene and dusty plagioclase crystals (up to 2 mm) are occupied by late-stage alkali-feldspar–plagioclase granophyric intergrowths (0·4–1·0 mm in size). Other late crystallization products are brown biotite and light green chlorite, which may partly rim the pyroxenes, apatite and Fe–Ti oxides, the last commonly exhibiting trellis textures formed by exsolution of ilmenite from magnetite (Fig. 2). Occasionally, small (0·6 mm) euhedral zircons are observed in association with the late-stage crystallization products.

Orthopyroxene grains vary in abundance from 25 to 35 vol. % (Table 3). They are strongly zoned, with colourless cores and brown rims corresponding to compositional zoning ranging from *mg*-number 84 to 60 [*mg*-number = $(100Mg/(Mg+Fe^{tot})]$, respectively. Most cores have *mg*-number in the range 76–80 (Table 5), whereas rim compositions depend markedly on the adjacent mineral. For instance, rims adjacent to clinopyroxene have *mg*-number 68–72 whereas rims in contact with plagioclase, or late-stage assemblages, are more Fe rich, with *mg*-number 60–65. Al_2O_3 contents are consistently

Table 2: PGE, sulphur and trace element analyses

Rock type:	Homogeneous Norite				Mottled Norite			Rubbly Norite									
Sample no.:	69894	70667	70688	70801	70661	70755	70788	70653	70683	70758	70766	70706	71892	71894	70783	71950	71986
PGE (p.p.b.)																	
Ir	0·46	0·41	0·11	0·25	1·1	0·1	0·06	2·2	0·9	1·1	1·1	0·9	0·16	0·04	0·3	0·3	0·9
Ru	1·7	1·6	1·4	1·9	7·0	2·9	1·5	21	6·0	10·0	8·5	3·0	1·6	1·3	3·0	1·0	4·0
Rh	n.d.	n.d.	n.d.	n.d.	5·0	n.d.	n.d.	65	5·0	14·0	4·5	15·0	n.d.	n.d.	6·0	1·0	2·0
Pt	24·7	24·7	20·4	17·3	31·0	31·1	26·8	130	22·0	23·0	13·0	50	20·5	15·7	9·0	12·0	26·0
Pd	12·4	12·1	6·6	7·5	15·0	5·8	6·7	1300	66	100	54	420	23·4	12·1	150	6·0	2·0
Au	0·3	0·42	1·3	1·6	14·0	1·3	1·4	62	8·0	8·0	4·0	23·0	2·8	2·3	25·0	1·0	1·0
mg-no.	62·3	71·0	67·8	63·7	70·4	71·7	67·9	74·6	70·4	72·0	71·2	69·6	66·4	57·1	68·8	62·8	71·8
Sulphur and trace elements (p.p.m.)																	
S	143	76	151	96	62	104	44	3813	1118	1092	254	4358	545	67	728	164	79
Ni	214	344	332	253	362	415	305	1405	661	802	442	1857	285	159	909	224	400
Cu	77	33	100	64	88	74	73	840	307	358	90	1798	96	98	557	70	68
Zn	84	87	83	91	89	87	88	92	111	92	95	142	91	85	76	86	105

Rock type:	High-Mg Tholeiites (HMT)						Fine-grained dykes			Fe-rich Tholeiite	Standard Komatiite	Chondrite C1
Sample no.:	65209	70533	70548	70612	71906	71947	70701	70709	71984	65098		
PGE (p.p.b.)												
Ir	0·6	0·3	0·16	0·2	0·22	0·02	0·3	0·3	0·09	0·018	0·8	540
Ru	2·6	0·6	0·83	0·8	2·08	0·68	0·7	0·2	0·92	n.d.	3·0	690
Rh	n.d.	n.d.	n.d.	n.d.	n.d.	n.d.	n.d.	n.d.	n.d.	n.d.	n.d.	200
Pt	17·1	10·5	9·7	18·4	13·2	11·0	14·8	15·2	13·8	6·1	8·0	1021
Pd	15·0	16·7	8·4	16·2	9·9	11·3	17·3	14·8	7·7	0·54	8·0	545
Au	3·2	1·7	1·8	4·6	1·8	1·7	2·3	3·3	2·0	0·21	0·6	152
mg-no.	68·6	67·8	68·3	57·0	68·8	58·8	59·4	56·8	59·1	41·3	81·7	
Sulphur and trace elements (p.p.m.)												
Ni	379	310	305	90	349	96	187	182	169	87	1477	
Cu	103	90	86	99	108	108	106	99	95	132	30	0·011
Zn	88	85	82	75	82	77	89	88	83	151	55	

PGE, sulphur and trace element analyses from various norite types and associated dykes. Ni abundance for C1 is from Palme *et al.* (1978) and C1 PGE concentrations (recalculated to 100% sulphide) are from Naldrett & Duke (1980). PGE and Au determined by fire assay and neutron activation analysis; S determined by LECO iodate titration; and trace elements determined by XRF. n.d., not determined. Before being normalized to chondrite, PGE were recalculated to 100% sulphide, assuming 38% S in sulphide liquid. A komatiite was used as internal standard.

Table 3: Selected High-Mg Tholeiite whole-rock analyses

Sample no.:	70533	70612	70688	70801	70653	70766	70661	70704	70709	71889
Rock type:	HMT	HMT	HN	HN	RN	RN	MN	MN	FGD	FGD
Sub-group:	I	Ia	II	II	IIa	IIa	II	II	II	II
SiO_2	51·80	54·58	55·40	55·14	55·84	54·93	55·97	56·72	55·92	56·15
TiO_2	0·60	0·67	0·56	0·52	0·39	0·44	0·55	0·64	0·74	0·71
Al_2O_3	11·36	13·28	10·51	11·12	6·81	8·26	9·30	10·33	13·00	12·64
Fe_2O_3	11·60	10·61	11·47	12·42	12·67	12·77	11·87	11·82	11·39	11·37
FeO	0·00	0·00	0·00	0·00	0·00	0·00	0·00	0·00	0·00	0·00
MnO	0·19	0·16	0·16	0·19	0·19	0·19	0·19	0·18	0·17	0·16
MgO	12·36	7·09	12·17	11·00	18·77	15·91	14·27	12·26	7·56	8·33
CaO	9·28	9·67	6·78	7·45	4·74	5·41	5·78	6·11	7·93	7·71
Na_2O	1·74	2·25	1·32	1·71	0·81	0·93	1·20	1·36	1·72	1·77
K_2O	0·59	0·96	0·96	0·96	0·62	0·72	0·92	1·09	1·33	1·21
P_2O_5	0·10	0·11	0·09	0·09	0·04	0·07	0·08	0·11	0·13	0·12
LOI	0·14	0·27	−0·04	−0·06	−0·12	0·24	−0·19	−0·23	0·16	0·06
Total	99·76	99·65	98·35	99·42	99·62	98·72	98·87	99·33	100·05	100·23
mg-no.	67·8	56·9	67·8	63·7	74·6	71·2	70·4	67·3	56·8	59·2
Ba	212	336	216	202	131	159	201	245	292	286
Rb	20	40	41	40	37	43	51	61	72	64
Nb	3	4	6	5	5	6	8	8	6	7
Sr	160	267	90	98	50	71	77	94	115	107
Zr	54	76	85	78	50	69	83	104	122	113
Y	18	15	19	14	11	11	21	19	22	22
Ni	311	92	332	253	1395	452	360	294	199	179
Cr	1225	373	1152	836	2104	1431	1509	1169	524	615
V	238	218	213	215	187	216	201	208	221	213
Sc	39	35	31	35	28	32	30	30	34	33
La	7·8	14	15	13·8	9·1	11	14·4	17	20·7	19·6
Ce	15·6	32	33	28·2	17·6	23	29·5	34	42·1	40·2
Pr	2·4	—	—	3·3	2·0	—	3·3	—	4·6	4·5
Nd	9·3	14	14	12·4	8·3	7	12·8	15	18·0	18·1
Sm	2·4	—	—	2·5	2·2	—	2·6	—	3·8	4·0
Eu	0·8	—	—	0·7	0·8	—	0·8	—	1·1	1·0
Gd	2·7	—	—	2·6	2·0	—	2·8	—	4·2	3·9
Dy	2·7	—	—	2·6	2·1	—	2·8	—	4·1	4·1
Er	1·7	—	—	1·5	1·3	—	1·8	—	2·3	2·3
Yb	1·6	—	—	1·4	1·2	—	1·4	—	2·0	2·1
Modal composition										
Ol	5	—	—	—	—		—	—	—	—
Opx	15	15	35	32	60	60	25	27	25	25
Cpx	30	25	15	12	10	6	15	10	10	15
Plag	40	40	30	40	8	20	40	40	60	50
Sp	<1	—	—	—	—	—	—	—	—	—
Bio	1	3	5	4	3	2	3	5	3	5
Granophyre	—	15	14	10	10	10	15	15	1	3
Opaques	4	2	1	2	8	2	2	3	1	2
CIPW norm wt %										
Qtz	5·58		7·41	5·26	4·94	5·84	7·04	8·66	9·22	8·88
Cpx	19·39	19·67	10·64	13·47	8·15	8·19	8·78	8·70	12·05	11·87
Opx	34·95	22·09	40·63	37·77	60·33	53·23	47·41	42·21	28·01	30·02
Ol	1·52									

High-Mg Tholeiite whole-rock analyses showing various rock types and sub-groups, including Homogeneous Norite (HN), Rubbly Norite (RN), Mottled Norite (MN), fine-grained dykes (FGD) and other High-Mg Tholeiite dykes (HMT). —, not determined. *mg*-number = $100Mg/(Mg + Fe^{tot})$. Major elements are given in wt % and trace elements in p.p.m.

Table 4: Selected microprobe analyses from sulphides, sulfarsenides and PGE minerals (sample number 70653)

Mineral:	Chalcopyrite			Pyrrhotite		Pentlandite		Sulpharsenide				Michenerite			
Rock type:	R-Norite														
S	34·80	34·92	34·66	39·22	38·89	32·97	32·59	18·54	19·68	19·85	19·73	0·01	0·02	0·04	0·03
Fe	30·71	30·77	35·33	58·95	59·34	30·19	30·06	5·48	5·38	5·19	6·30	0·76	1·66	1·68	0·71
Ni	0·00	0·03	0·04	1·37	1·55	36·02	36·01	23·70	11·72	7·50	11·58	0·01	0·26	0·29	0·02
Cu	33·48	33·54	29·88	0·01	0·01	0·07	0·06	0·67	0·14	0·12	0·10	0·86	0·60	0·36	0·80
As	0·00	0·09	0·08	0·00	0·02	0·08	0·01	43·67	42·63	42·73	43·02	0·00	0·00	0·00	0·00
Pd	0·00	0·03	0·00	0·00	0·00	0·00	0·01	0·17	1·06	0·47	1·25	25·27	24·64	24·99	25·58
Te	0·00	0·00	0·02	0·00	0·03	0·04	0·02	0·01	0·01	0·00	0·01	29·61	33·90	33·58	29·84
Co	0·00	0·00	0·00	0·00	0·01	0·56	0·54	6·74	17·41	23·06	16·78	0·00	0·13	0·18	0·00
Pt	0·15	0·12	0·00	0·08	0·00	0·02	0·00	0·02	0·00	0·11	0·00	0·89	0·57	0·67	0·90
Bi	0·03	0·03	0·19	0·18	0·02	0·09	0·00	0·00	0·00	0·00	0·00	44·03	38·09	38·69	44·11
Total	99·18	99·52	100·20	99·80	99·89	100·05	99·32	99·00	98·04	99·04	98·77	101·44	99·88	100·48	101·97
Atom proportions															
S	0·990	0·989	0·975	1·048	1·039	0·923	0·919	0·951	1·012	1·008	1·008	0·000	0·001	0·002	0·001
Fe	0·516	0·515	0·587	0·930	0·936	0·499	0·501	0·166	0·163	0·156	0·190	0·019	0·041	0·041	0·018
Ni	0·000	0·000	0·001	0·021	0·023	0·566	0·570	0·683	0·338	0·214	0·332	0·000	0·006	0·007	0·000
Cu	0·494	0·493	0·436	0·000	0·000	0·001	0·001	0·018	0·004	0·003	0·003	0·019	0·013	0·008	0·018
As	0·000	0·001	0·001	0·000	0·000	0·001	0·000	0·986	0·965	0·955	0·967	0·000	0·000	0·000	0·000
Pd	0·000	0·000	0·000	0·000	0·000	0·000	0·000	0·003	0·017	0·007	0·020	0·333	0·318	0·321	0·336
Te	0·000	0·000	0·000	0·000	0·000	0·000	0·000	0·000	0·000	0·000	0·000	0·326	0·364	0·360	0·326
Co	0·000	0·000	0·000	0·000	0·000	0·009	0·009	0·193	0·501	0·655	0·480	0·000	0·003	0·004	0·000
Pt	0·001	0·001	0·000	0·000	0·000	0·000	0·000	0·000	0·000	0·001	0·000	0·006	0·004	0·005	0·006
Bi	0·000	0·000	0·001	0·001	0·000	0·000	0·000	0·000	0·000	0·000	0·000	0·296	0·250	0·253	0·295
Sum	2·000	2·000	2·000	2·000	2·000	2·000	2·000	3·000	3·000	3·000	3·000	1·000	1·000	1·000	1·000

Microprobe analyses from base metal sulphides, sulpharsenides and PGE minerals from Rubbly Norite. Number of atoms calculated for 2, 3 and 1 atom per formula unit. Analytical conditions: CAMECA SX-50 microprobe; 20 kV; 100 nA.

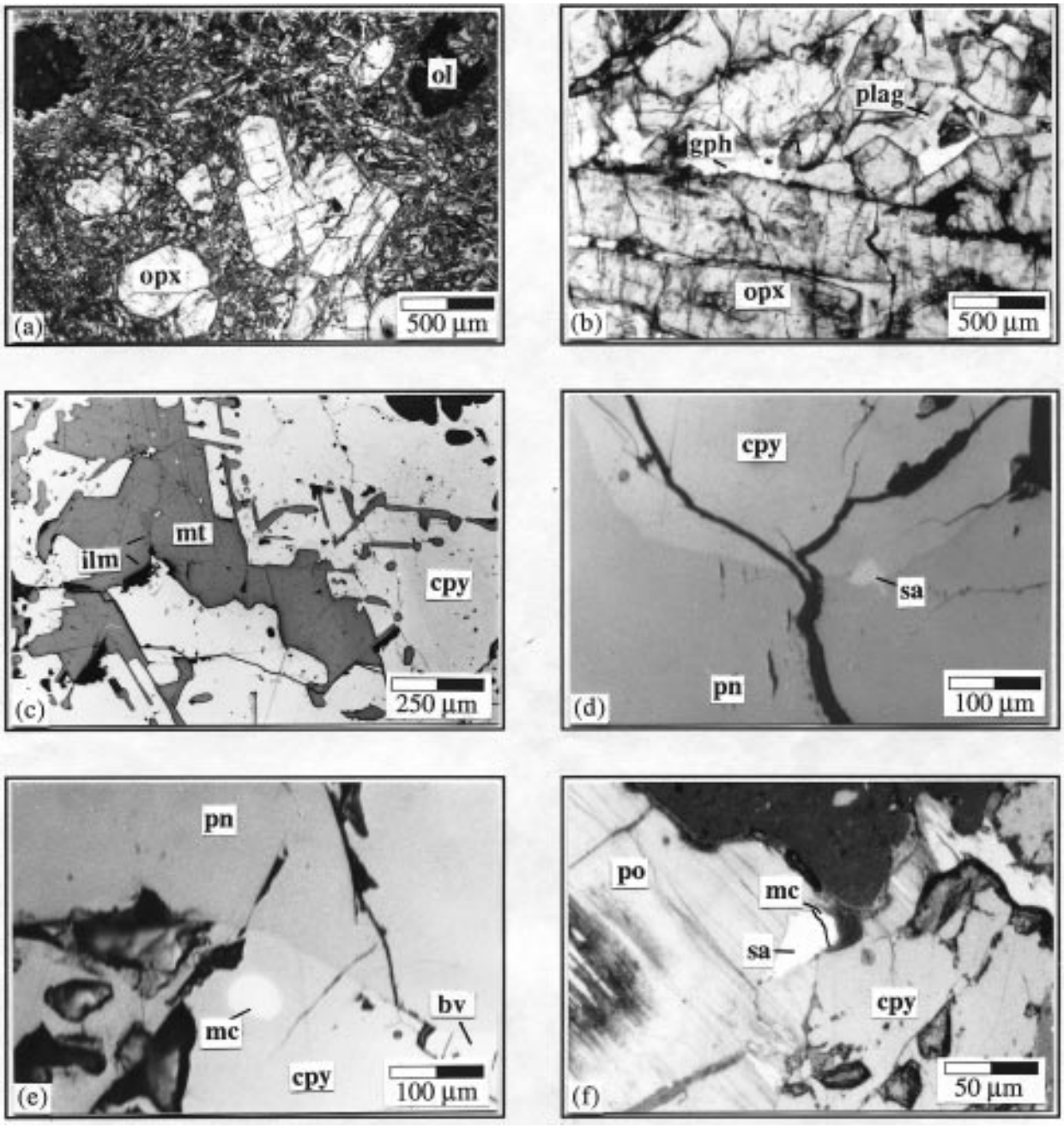

Fig. 2. Photomicrographs of: (a) HMT dyke, showing chilled margin with orthopyroxene (opx) and olivine (ol) phenocrysts in a fine-grained groundmass consisting mainly of clinopyroxene and plagioclase. (b) Cumulus orthopyroxene (opx) in the Rubbly Norite. (c) Ilmenite (ilm) exsolution lamellae parallel (111) in magnetite (mt). (d) Chalcopyrite (cpy) and pentlandite (pn) with sulpharsenide (sa). (e) Michenerite (mc) inclusion in chalcopyrite—partial bravoite (bv) border between chalcopyrite and pentlandite. (f) Chalcopyrite, pyrrhotite (po) and interstitial sulpharsenide partly mantled by michenerite.

between 1·1 and 1·7 wt %, rarely exceed 2 wt %, and show no zoning. CaO generally increases from 1·0 to 2·2 wt % from core to rim, with the exception of some orthopyroxenes which have rim compositions as low as *mg*-number 60 and CaO contents as high as 1·6 wt %.

The modal abundance of intercumulus clinopyroxene occasionally exceeds 10 vol % (Table 3). The compositional variation of clinopyroxene is much more limited than that of orthopyroxene, with, for example, *mg*-number varying from 73·3 in cores to 61·5 at crystal

Table 5: Selected electron microprobe analyses from pyroxenes, olivines and spinels

	Orthopyroxene						Clinopyroxene					Olivine		Spinel		
Sample no.:	70667	70661	70653	71952	70709	70548	70667	70661	70653	70623	70548	71952	70533	71952	71952	70538
Pos. of anal.:	core	core	core	core	core	core	core	core	core	rim	rim	core	core	rim	core	core
Rock type:	HN	MN	RN	RN	FGD	HMT	HN	MN	RN	FGD	HMT	RN	HMT	RN	RN	HMT
SiO_2	56·10	56·27	56·10	55·46	55·25	53·70	54·01	52·88	52·52	52·67	51·13	40·86	39·57	0·01	0·05	0·35
TiO_2	0·00	0·000	0·000	0·04	0·000	0·04	0·000	0·28	0·000	0·20	0·30	0·000	0·000	0·01	0·29	0·14
Al_2O_3	0·97	0·87	1·07	1·92	0·84	1·99	0·80	1·85	2·71	2·40	3·88	0·000	0·000	36·15	13·38	14·29
Cr_2O_3	0·58	0·48	0·57	0·73	0·46	0·86	0·00	0·37	0·75	0·44	0·17	0·00	0·03	26·74	48·26	45·08
Fe_2O_3														8·53	4·70	6·94
FeO	10·50	10·38	11·01	6·45	14·11	10·20	6·89	10·60	7·93	12·84	10·75	9·70	14·31	10·56	20·53	26·36
NiO	0·00	0·00	0·00	0·11	0·00	0·21	0·00	0·00	0·00	0·22	0·21	0·38	0·32	0·12	0·18	0·00
MnO	0·00	0·00	0·00	0·17	0·00	0·00	0·00	0·00	0·00	0·00	0·03	0·16	0·14	0·31	0·18	0·00
MgO	30·77	30·91	30·07	33·66	28·25	29·99	15·59	16·76	16·61	19·44	17·42	49·21	45·02	17·43	7·86	4·73
CaO	1·08	1·09	1·18	0·75	1·08	2·45	22·71	17·03	19·38	11·78	15·82					
Na_2O	0·00	0·00	0·00	0·00	0·00	0·00	0·00	0·20	0·15	0·00	0·24					
Total	100·00	100·00	100·00	99·29	99·99	99·44	100·00	99·97	100·05	99·99	99·95	100·31	99·38	99·87	95·44	97·88
Cations on the basis of 6 oxygens												*Cations on the basis of 4 oxygens*				
Si	1·975	1·979	1·979	1·930	1·978	1·904	1·991	1·956	1·932	1·940	1·883	0·999	0·998	0·000	0·000	0·000
Ti	0·000	0·000	0·000	0·001	0·000	0·001	0·000	0·008	0·000	0·006	0·008	0·000	0·000	0·000	0·007	0·004
Al	0·040	0·036	0·044	0·079	0·035	0·083	0·035	0·081	0·117	0·104	0·169	0·000	0·000	1·215	0·546	0·583
Cr	0·016	0·013	0·016	0·020	0·013	0·024	0·000	0·011	0·022	0·013	0·005	0·000	0·000	0·602	1·317	1·230
Fe^3	0·000	0·000	0·000	0·039	0·000	0·082	0·000	0·000	0·008	0·000	0·061	0·000	0·000	0·183	0·122	0·180
Fe^2	0·309	0·305	0·325	0·149	0·422	0·220	0·212	0·328	0·236	0·395	0·270	0·198	0·302	0·251	0·593	0·761
Mn	0·000	0·000	0·000	0·003	0·000	0·006	0·000	0·000	0·000	0·007	0·007	0·003	0·003	0·003	0·005	0·000
Ni	0·000	0·000	0·000	0·005	0·000	0·000	0·000	0·000	0·000	0·000	0·001	0·009	0·008	0·007	0·005	0·000
Mg	1·615	1·621	1·582	1·746	1·508	1·585	0·857	0·924	0·911	1·067	0·956	1·792	1·692	0·739	0·404	0·243
Ca	0·041	0·041	0·045	0·028	0·041	0·093	0·897	0·675	0·764	0·465	0·624	0·000	0·000	0·000	0·000	0·000
Na	0·000	0·000	0·000	0·000	0·000	0·000	0·000	0·014	0·011	0·000	0·017	0·000	0·000	0·000	0·000	0·000
Sum	3·997	3·996	3·991	4·000	3·998	4·000	3·992	3·997	4·000	3·996	4·000	3·001	3·002	3·000	3·000	3·000
mg-no.	83·9	84·1	83·0	91·9	78·1	84·7	80·1	76·5	78·9	73·0	74·3	90·0	84·9	74·6	40·6	24·2
cr-no.														33·1	70·7	67·9

Selected mineral analyses from various norite types. *mg*-number(silicates) = 100Mg/(Mg + Fe^{tot}); *mg*-number(spinel) = 100Mg/(Mg + Fe^{2+}); *cr*-number = 100Cr/(Cr + Al). Fe determination as FeO: Fe^{3+} and Fe_2O_3 calculated from stoichiometry. HN, Homogeneous Norite; RN, Rubbly Norite; MN, Mottled Norite; FGD, fine-grained dykes; HMT, other High-Mg Tholeiite dykes.

rims (Table 5). Where clinopyroxene is in contact with orthopyroxene, rims have an average *mg*-number of 70. Plagioclase is cloudy, owing to small opaque inclusions. Plagioclase is strongly zoned, usually from An_{80} cores to An_{50} rims although some rim compositions are as sodic as An_{32}.

Mottled Norite

The Mottled Norite occurs occasionally as narrow bands between the Homogeneous Norite and the Rubbly Norite. It constitutes ~10% of the exposed outcrop (Fig. 1d). This rock type is most abundant in the southern outcrops of the Taynaya Bay region and is distinguished from the Homogeneous Norite by its large, evenly distributed glomeroporphyritic aggregates of feldspars and quartz. The crystal aggregates are granophyric intergrowths of orthoclase, plagioclase and quartz. These granophyric intergrowths make up 15–20 vol. %, compared with only 10–15 vol. % in the Homogeneous Norite. The plagioclase intergrown with alkali-feldspar in these aggregates ranges in composition from An_{52} to An_{60}, and the alkali-feldspar varies from $Or_{92}Ab_{7·2}An_{0·8}$ to $Or_{84}Ab_{13·6}An_{2·4}$. Small (up to 2 mm) apatite needles are also associated with the plagioclase–K-feldspar–quartz intergrowths.

Cumulus orthopyroxene are up to 8 mm long. They are strongly zoned from cores of *mg*-number 84·5 to rims of *mg*-number 57 (Table 5).

Subhedral orthopyroxene is often rimmed by inverted pigeonite. Intercumulus subhedral clinopyroxene occupies between 5 and 15 vol. % (average 1·6 mm in size). Its composition varies from *mg*-number 78·5 for the core to *mg*-number 64 for the rim (Table 5). Biotite and chlorite represent 1–3 vol. %, whereas iron–titanium oxides and sulphides never exceed 2 vol. % (Table 3).

Rubbly Norite

The Rubbly Norite is the most heterogeneous norite unit and occurs in small elongate bodies at the outer margins of the ring complex that vary in size, from only a few metres in width up to 30 m. The largest body in the Taynaya Bay region (Fig. 1d) reaches a maximum width of 20 m and extends over a linear distance of 400 m. The Rubbly Norite is characterized by irregularly shaped bronzite-rich zones, which give the rock its typical brownish colour in hand-specimen. This inhomogeneity is further enhanced by the presence of enstatite nodules up to 0·6 m in diameter and sulphide-rich zones. On exposure to weathering, these sulphide-rich zones become an obvious green to reddish colour. In marginal zones, adjacent to country rocks, crustal xenoliths are common, and include both sapphirine- and diopside-bearing xenoliths. Owing to the heterogeneity of the Rubbly Norite, petrographic features are more complex than in the other norite units. The Rubbly Norite is dominated by orthopyroxene, at up to 65 vol. % (Table 3). Euhedral to subhedral orthopyroxenes, of >1 cm in length, show orthocumulate to adcumulate textures. The mineral chemistry of the orthopyroxenes is similar to that in the other norite units, ranging from cores of *mg*-number 85 to rims of *mg*-number 62. Some orthopyroxenes from cognate enstatite-rich nodules (Kuehner, 1989) yield cores of *mg*-number 91·9 (Table 5). Olivines occurring within these enstatites generally have cores of *mg*-number 85–87. However, some more magnesian olivines were found with cores of *mg*-number 88·3 and 90 [Harley & Christy (1995) and Seitz (1991), respectively]. Spinels which are associated with these olivines are strongly zoned, with cores of *cr*-number [100Cr/(Cr+Al)] 40 and rims of *cr*-number 75 (Table 5).

Intercumulus clinopyroxene (~5 vol. %) has a compositional range similar to that in the other norite varieties. The amount of plagioclase (10 vol. %) is less than in the Homogeneous Norite (Table 3). Compositions vary from An_{68} cores to An_{62} rims, though plagioclase intergrowths with K-feldspar are more sodic in character ($An_{50–54}$). With decreasing plagioclase content in the Rubbly Norite, the granophyric patches become less abundant also (5–10 vol. %). These intercumulus granophyric patches occupy areas up to 4 mm in diameter.

Fine-grained dykes

A number of fine-grained dykes occur in proximity to the NRC. The more slowly cooled dyke interiors exhibit textural and mineralogical similarities to the Homogeneous Norite. The dykes are orthopyroxene-phyric with 15–25 vol. % phenocrysts (Table 3). Euhedral orthopyroxene phenocrysts (up to 2·5 mm in length) commonly form glomeroporphyritic clusters. Orthopyroxene occasionally is rimmed by clinopyroxene. Orthopyroxene has pronounced zoning with cores of *mg*-number 83·3 and rims of *mg*-number 56 (Table 5). Clinopyroxene exsolution at the orthopyroxene rims ranges between *mg*-number 62 and 70. Al_2O_3 in orthopyroxene is relatively constant, whereas CaO increases with increasing differentiation, from *mg*-number 92 to 68, and then decreases from *mg*-number 68 to 48. The inflection in CaO contents in orthopyroxene is consistent with the onset of clinopyroxene crystallization at $mg\text{-number}_{opx}$ of 68. Al_2O_3 and CaO in clinopyroxene show no systematic variation with decreasing *mg*-number, whereas TiO_2 increases slightly. Orthopyroxene and clinopyroxene in the fine-grained dykes overlap compositionally with those from the norites.

The groundmass consists of plagioclase (~50 vol. %), clinopyroxene (5–15 vol. %), biotite, a granophyric intergrowth of quartz and alkali-feldspar, Fe–Ti oxides and sulphides (Table 3). Plagioclase compositions are intermediate, ranging from An_{65} cores to An_{53} rims.

High Magnesium Tholeiite dykes

These dykes are olivine- and orthopyroxene-phyric. Anhedral olivine crystals in chilled margin samples (up to 0·6 mm in size) either are rimmed by kelyphite, comprising opaque minerals and orthopyroxene, or are completely replaced by orthopyroxene and magnetite symplectites. Coarser-grained samples from the dyke interior frequently contain subhedral to anhedral olivine crystals up to 1·4 mm, which are always mantled by orthopyroxene. Olivine phenocrysts show no zonation in Mg and Fe, revealing compositions of *mg*-number 85 (Table 5). The modal abundance of olivine phenocrysts never exceeds 10 vol. %.

Glomeroporphyritic clusters of euhedral orthopyroxene phenocrysts, up to 2 mm in size, are more abundant than olivine, with modal abundances between 10 and 30 vol. % (Table 3). Sub-ophitic textures are common, with small (0·1–0·3 mm) plagioclase laths being partly or entirely enclosed by orthopyroxenes. Compositions of enclosed plagioclase range from $An_{70·7}$ cores to $An_{61·5}$ rims. The orthopyroxene phenocrysts show strong zonation from cores of *mg*-number 84·5 to rims of *mg*-number 75 (Table 5). A maximum of *mg*-number 88 core composition has been described by Kuehner (1989). Narrow (0·02 mm wide) inverted pigeonite rims occasionally occur around orthopyroxenes.

Spinels commonly occur as small (0·025 mm) euhedral to anhedral inclusions in orthopyroxene phenocrysts. They are unzoned and chrome rich in character, with *cr*-number between 69·9 and 72·9 (Table 5).

The groundmass consists mainly of plagioclase, clinopyroxene and orthopyroxene, with approximate abundances of 40, 20 and 10 vol. %, respectively. Minor phases are biotite, apatite and opaques (magnetite, ilmenite and subordinate sulphides). Groundmass orthopyroxenes have a wide range in composition, with typically *mg*-number 65 in cores and becoming less magnesian (*mg*-number 59) towards the rims. Plagioclase is only present in the groundmass and has a compositional range of $An_{69·8}$ for cores and $An_{47·1}$ for rims.

Oxide, sulphide and PGE mineralogy

Modal abundances of opaque minerals increase from to ~2 vol. % in the HMT dykes, fine-grained dykes, Homogeneous Norite and Mottled Norite to ~8 vol. % in the Rubbly Norite. Whereas oxide minerals (magnetite and ilmenite) are dominant in the former three rock types, they are subordinate to sulphides in the Rubbly Norite. Sulphides occur as disseminated blebs (~0·1–0·2 mm in diameter) throughout the NRC, and additionally as irregular globular patches (2–3 cm in diameter) often associated with other pyroxenite nodules in the Rubbly Norite. They invariably occupy intercumulus sites surrounded by either orthopyroxene phenocrysts or, more commonly, late-stage quartz and alkali-feldspar intergrowths. These relationships, and the observation that sulphides sometimes enclose magnetite and ilmenite, indicate a late-stage origin during crystallization of the norites. The sulphide globules are composites of pyrrhotite (FeS), chalcopyrite ($CuFeS_2$), pentlandite [$(Fe,Ni)_9S_8$] and bravoite [$(Fe,Ni)S_2$]. Modal abundances of these phases in the Rubbly Norite vary from sample to sample; however, pyrrhotite is generally more abundant than chalcopyrite and, in turn, pentlandite (Table 6). Bravoite is only a minor phase which, when present, occurs as thin (10–20 μm) borders between pyrrhotite and pentlandite. Microprobe analyses of the main sulphides are generally stoichiometric (Table 4), except for pyrrhotite, which is commonly between Fe_7S_8 and Fe_8S_9. Trace elements were not detected in the sulphide phases, with the exception of up to 0·15 wt % platinum in some

Table 6: Opaque mineral assemblages in the Rubbly Norite

		Ideal formula	Averaged abundances (vol. %)*
Sulphides			
Pyrrhotite	(po)	$Fe_{1-x}S$	3·3
Pentlandite	(pn)	$(Fe,Ni)_9S_8$	1·5
Chalcopyrite	(cpy)	$CuFeS_2$	2·3
Bravoite	(bv)	$(Ni,Fe,Co)S_2$	<0·1
Sulpharsenides	(sa)		
Arsenopyrite		FeAsS	
Gersdorffite		NiAsS	<0·1
Cobaltite		CoAsS	
Tellurides			
Michenerite	(mc)	PdBiTe	<0·1
Oxides			
Magnetite	(mt)	$FeFe_2O_4$	0·5
Ilmenite	(ilm)	$FeTiO_3$	1·1

Base metal sulphide (BMS), sulpharsenide, telluride and oxide mineral assemblages in Rubbly Norite.
*Average volume per cent (estimated) sulphide is given relative to the whole-rock mineral abundances. Sulpharsenides always occur as solid solutions between the end-members arsenopyrite, gersdorffite and cobaltite.

chalcopyrites. Sulpharsenides and tellurides were found in the more sulphide-rich samples, occurring both as minute inclusions (up to 20 μm in diameter) in chalcopyrite and pyrrhotite, and along grain boundaries within globular sulphides. The sulpharsenides are solid solutions between arsenopyrite (FeAsS), gersdorffite (NiAsS) and cobaltite (CoAsS), ranging from $Ni_{0·21}Co_{0·65}Fe_{0·16}$ to $Ni_{0·68}Co_{0·18}Fe_{0·16}$. These compositions reflect high temperatures of formation, corresponding to experimentally determined isotherms between 550 and 600°C in the FeAsS–NiAsS–CoAsS system (Klemm, 1965).

Michenerite, a palladium–bismuth-telluride, is the only PGE mineral observed in the norite. It occurs as tiny discrete grains (up to 12 μm in diameter) associated with sulpharsenides and as inclusions in chalcopyrite (see Fig. 2). Compositions are near $Pd_{0·34}Bi_{0·30}Te_{0·36}$ (Table 4). Metallic Pt has been observed as minute inclusions within chalcopyrite. Traces of Pd and occasionally Pt detected in sulpharsenides and chalcopyrites (Table 4) could arise from the presence of minute inclusions within these phases. However, in these particular cases the presence of metallic Pd and Pt inclusions was not confirmed by back-scattered imaging; this suggests that both palladium and platinum may also be solid solution components in sulpharsenides and chalcopyrites. Traces of Pd and Pt in pendlandite were not detected.

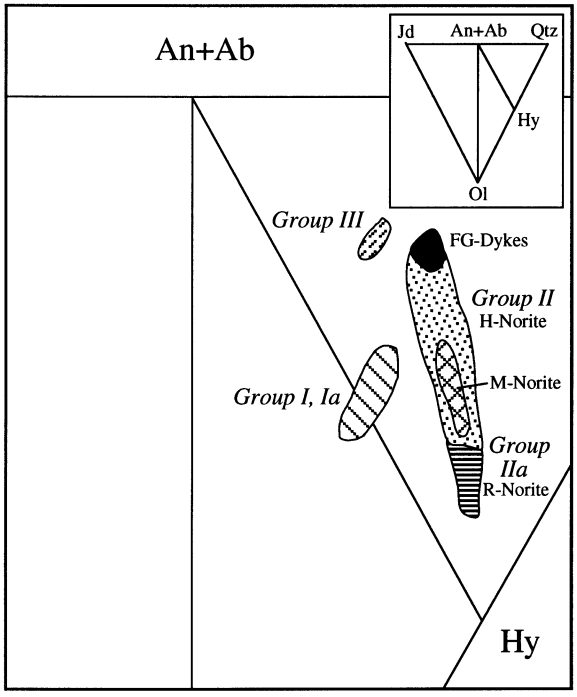

Fig. 3. Composition of HMT from the Vestfold Hills projected from diopside onto the plane (Jd+CaTs)–Ol–Qtz of the basalt tetrahedron following Green (1970) ($Fe_2O_3/FeO = 0·1$).

GEOCHEMICAL CHARACTERISTICS

Selected HMT whole-rock analyses are presented in Table 3. The Vestfold Hills HMT dykes have relatively high SiO_2 (52–57 wt %) and MgO (7–18 wt %), and low TiO_2 (0·38–0·74 wt %). Compositions vary from olivine normative (9·1 wt %) to quartz normative (10·8 wt %). The compositional spectrum extends from olivine- and orthopyroxene-phyric dykes with >9% MgO to include orthopyroxene-phyric 'fine-grained dykes' with ~7–8% MgO (Table 3).

This compositional spectrum is illustrated in Fig. 3, where all analysed samples are projected from diopside onto the base of the basalt tetrahedron, following Green (1971). Three distinct compositional groups are apparent (Fig. 3)—one group straddling the boundary between olivine and quartz normative fields, and two separate quartz normative groups. The quartz normative, norite types define a trend along a hypersthene control-line. Compositions become progressively less hypersthene normative from the Rubbly Norite through the Mottled Norite to the Homogeneous Norite.

Fine-grained dykes associated with the norite reveal compositional variations similar to those of the Homogeneous Norite, and have similar modal orthopyroxene abundances (Table 3).

Trace element patterns show enrichment of large ion lithophile elements (LILE; Ba, Rb, K) and light REE (LREE) relative to the high-field strength elements (HFSE) Nb and Ti (Fig. 4). All groups exhibit pronounced negative anomalies in Nb, P and Ti, when normalized against 'primitive mantle' (Fig. 4), as inferred by Sun *et al.* (1989). The absence of a negative Sr anomaly readily distinguishes Group I from the Group II, IIa and III dykes. The Group II and IIa dykes in turn, can be separated from Group III by Rb enrichment relative to Ba and K in Group II and IIa dykes, with primitive mantle normalized Rb/Ba_n ratios in the range 0·8–0·9 for Group III, 1·2–2·5 for Group II and 1·1–1·5 for Group IIa. Group III has different $(Sr/Nd)_n$ ratios from Group I, but similarly low $(Sr/Nd)_n$ ratios compared with Groups II and IIa. On the basis of geochemistry, mineralogy and crosscutting relationships, the following subdivision of the Vestfold Hills HMT can be made:

Group I—olivine- and orthopyroxene-phyric tholeiite;

Group Ia—orthopyroxene-phyric tholeiite;

Group II—orthopyroxene-phyric tholeiites including the Homogeneous Norite, Mottled Norite and associated fine-grained dykes;

Group IIa—orthopyroxene-phyric tholeiites including the Rubbly Norite;

Group III—orthopyroxene-phyric tholeiite.

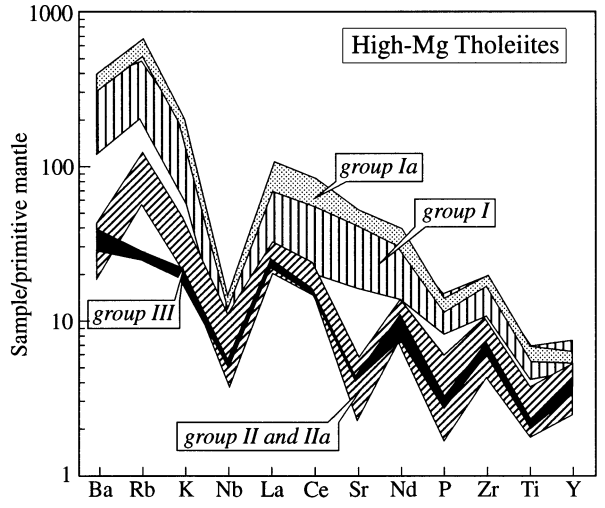

Fig. 4. Incompatible multi-element diagram for various HMT from the Vestfold Hills, distiguishing between Groups I, Ia, II, IIa and III. Data are normalized to primitive mantle after Sun & McDonough (1989).

Whereas Groups I, Ia, II and IIa were emplaced in succession (becoming younger with increasing number), Group III tholeiites are younger than Group I but their relationship to Groups II and IIa has not yet been established.

Ni, Cu, Zn, PGE AND S ABUNDANCES IN THE VESTFOLD HILLS DYKES

The PGE concentrations in the various norite types of the NRC, the HMT and the fine-grained dyke suite are given in Table 4 . Average PGE concentrations in the fine-grained and HMT dykes are remarkably uniform, with ~15 p.p.b. Pd, 10–18 p.p.b. Pt, 0·2–0·6 p.p.b. Ir and 2–5 p.p.b. Au (Table 4). Ruthenium concentrations are slightly more variable, ranging between 0·2 and 2·6 p.p.b. The PGE are also uniform in the Homogeneous Norite, but are 1–5 times higher than concentrations in the dykes. The Rubbly Norite, in contrast, has highly variable, and, on average, much higher PGE concentrations, ranging up to p.p.m. values for Pd.

Sulphur, Ni, and Cu in the HMT display similar systematics to the PGE, with abundances being highly variable and generally much greater in the Rubbly Norite (Table 4). S concentrations in the Rubbly Norite range from 80 to 4400 p.p.m., whereas the abundances in the Homogeneous and Mottled Norite are consistently low, between 45 and 150 p.p.m. Chilled margin compositions from the HMT dykes have S concentrations between 180 and 450 p.p.m. Samples 70533 (Group I), 70709 and 70701 (Group II), with 182, 194 and 256 p.p.m. S, respectively, are very S undersaturated. Group Ia samples 70612 and 65209 have slightly more elevated S contents of 375 and 449 p.p.m, respectively.

Zinc abundances are notable for being more or less uniform in all the analysed samples. The Cu, Ni, Zn, PGE and S abundances of a young (1380 Ma) Fe-rich tholeiite dyke (FRT) from the Vestfold Hills were analysed for comparative purposes (Table 4). The PGE concentrations are very low (Pd 0·54 p.p.b. and Pt 6·1 p.p.b.) whereas S, Cu and Zn are relatively high, at 1796, 132 and 151 p.p.m., respectively.

PARTIAL MELTING, CRYSTAL FRACTIONATION AND SULPHIDE SEGREGATION

To evaluate possible controls on PGE abundances by sulphide distribution in the HMT suite, the PGE were plotted against S as illustrated in Fig. 5a–d. A strong positive trend is observed between Pd and S, and between Pt and S at S contents >150 p.p.m. However, only weak positive trends exist between the other PGEs and S, being 'strongest' within the Rubbly Norite. The Homogeneous and Mottled Norite units are notable, for they consistently fall off these trends toward relatively high PGE abundances at low S contents.

The positive trends between Pt and S (Fig. 5a) and Pd and S (Fig. 5b), particularly in the Rubbly Norite, indicate that they are hosted by sulphides, which occur as disseminations, globules and lenses in the Rubbly Norite. The constant Pd contents and their lack of correlation with S within the dyke samples (including fine-grained dykes and HMT) clearly indicate that precipitation and redistribution of a sulphide phase does not control PGE variation in those samples, nor can such a process account for the position of the Homogeneous and Mottled Norite units relative to the Rubbly Norite and the dykes.

PGE abundances in the Vestfold Hills HMT, recalculated on a 100% sulphide basis and normalized to C1 chondrite values following Naldrett *et al.* (1979), are plotted on a multi-element diagram in Fig. 6a. This plot illustrates essentially parallel patterns for the entire HMT suite, and a 100-fold increase in normalized abundances from Ir to Pd and Au, and even higher normalized Cu abundances. A salient feature of the data is that the Homogeneous and Mottled Norite units plot well above the fine-grained dykes and Rubbly Norite patterns. Another notable feature is the anomalously high, normalized Pd abundances relative to Pt and Au in most Rubbly Norite samples (Fig. 6a).

For comparison, 'average' chondrite-normalized PGE patterns for the Rubbly Norite and dyke chilled margin samples with the patterns of selected basalt types and PGE-mineralized magmatic bodies are illustrated in Fig.

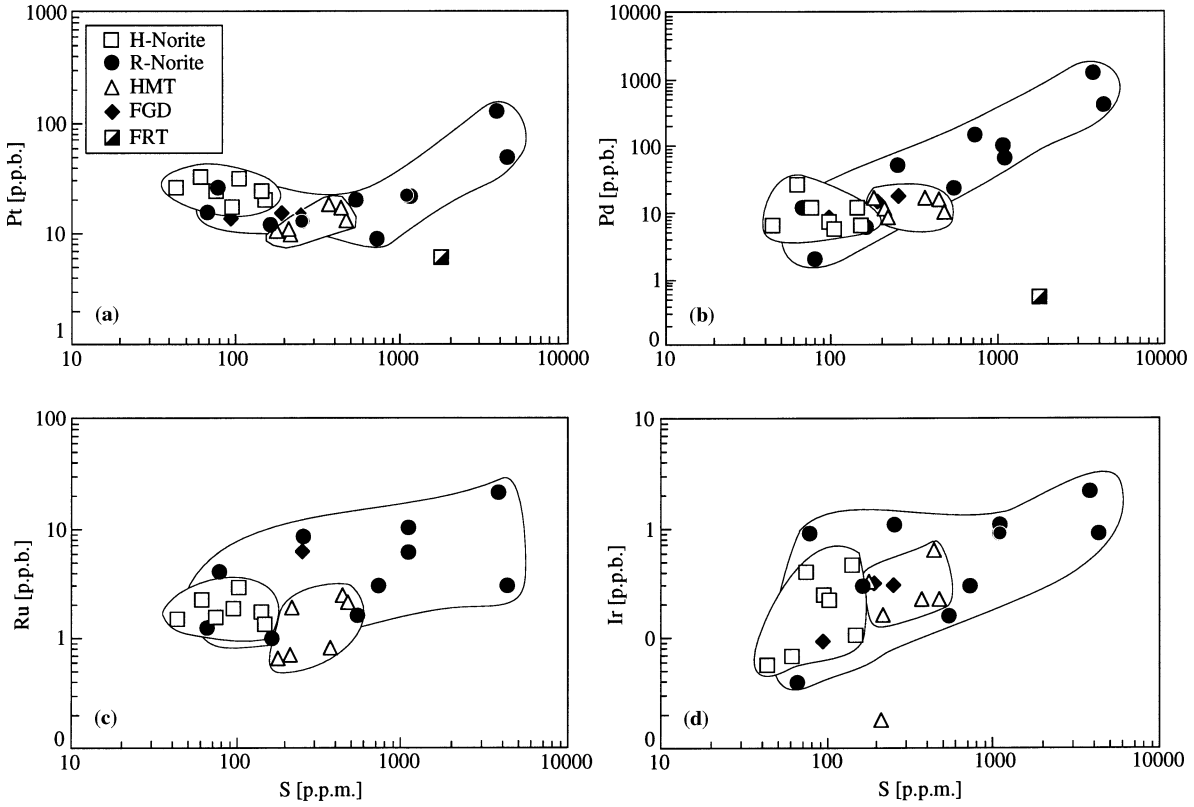

Fig. 5. PGEs Pt, Pd, Ru and Ir (p.p.b.) plotted vs S (p.p.m.) from various norite types, associated fine-grained dykes and HMT dykes.

6b. The Pd/Pt ratios of the mineralized samples of the Rubbly Norite are up to 10 times greater than the Pd/Pt ratios of the HMT dykes.

The Vestfold HMT have very similar patterns to komatiites, flood basalts and Sudbury, with a pronounced positive Pd anomaly, and high Pd/Pt ratios (up to 16), but are characterized by much higher normalized abundances (note that this is relative to S). In contrast, the Vestfold Hills patterns are very unlike that of the Stillwater complex, which has much greater normalized abundances of PGE and displays relatively large depletions in Au and Cu, and are also unlike that of the Merensky Reef, which is flat from Pt to Cu.

Variation in the ratios of PGE and other metals, which are subject to differing chemical behaviour, offers a potentially powerful means for illustrating and distinguishing the different processes which may control the abundances of these elements (Barnes *et al.*, 1988). Selected metal ratios of individual HMT samples are plotted in Fig. 7a and b. Also shown are vectors which indicate partial melting, fractionation or accumulation trends for various ferromagnesian or sulphide phases. The compositional fields of PGE reefs in layered intrusions, the mantle and several major basalt types are also shown for comparison. In terms of Pd/Ir vs Ni/Cu variation (Fig. 7a), the HMT form a dispersed trend, subparallel to both the partial melting and to olivine (and orthopyroxene) + chromite controlled differentiation vectors. In terms of Ni/Pd vs Cu/Pd variation, which is better able to distinguish between sulphide and silicate fractionation processes (see vectors in inset to Fig. 7b), a relatively tight trend is formed by the Rubbly Norite samples, which corresponds to sulphide accumulation and fractionation. It is further notable that in both diagrams the bulk of the HMT plot within the fields of layered intrusions and SHMB, and that the PGE-rich Rubbly Norite samples extend toward and overlap with PGE reef compositions.

PARENTAL MAGMAS

A cumulative origin was proposed by Seitz (1991) for the Rubbly Norite and the Mottled Norite. This is supported petrographically by the high modes of up to 65 vol. % orthopyroxene in the Rubbly Norite. Besides the accumulation of orthopyroxene, cognate pyroxenite nodules and sulphides are concentrated within the Rubbly Norite. The Mg-rich nature of orthopyroxenes and olivines (*mg*-number 92 and 90, respectively) in the cognate

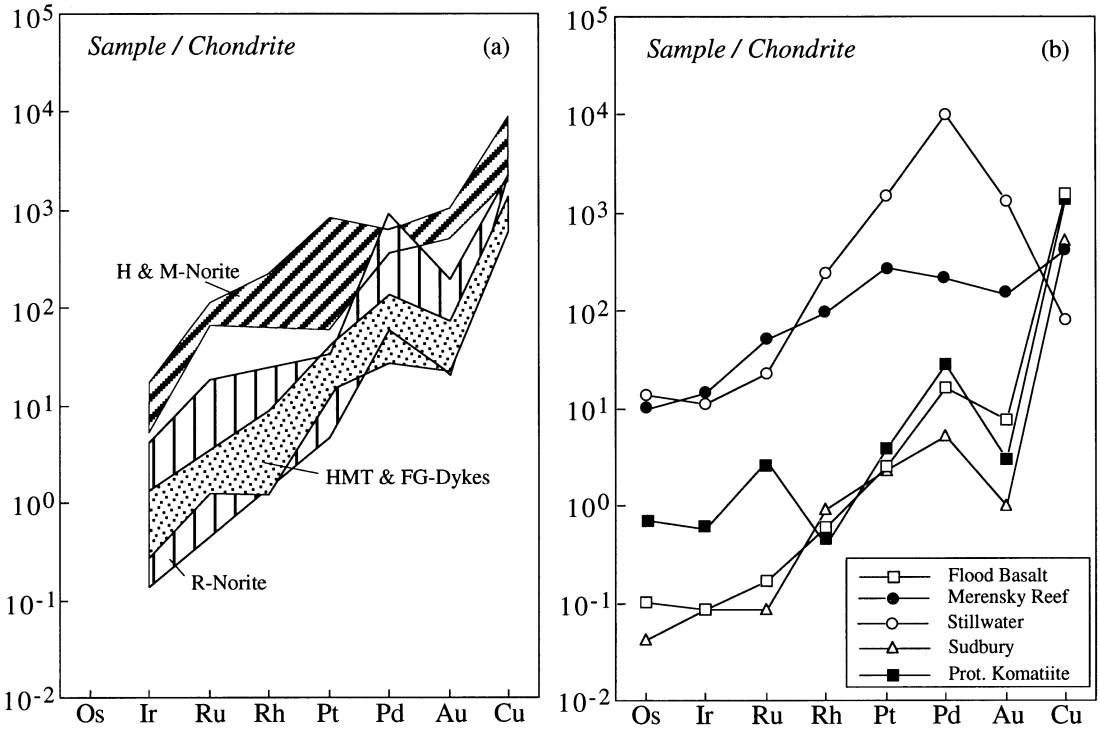

Fig. 6. Chondrite-normalized PGE patterns from the Vestfold Hills HMT and norites (a) in comparison with flood basalts, Merensky Reef, Stillwater, Sudbury and Proterozoic komatiite (b). Data are taken from Naldrett (1981). Before normalization to chondrite, PGE were recalculated to 100% sulphide, assuming 38% S in the sulphide liquid.

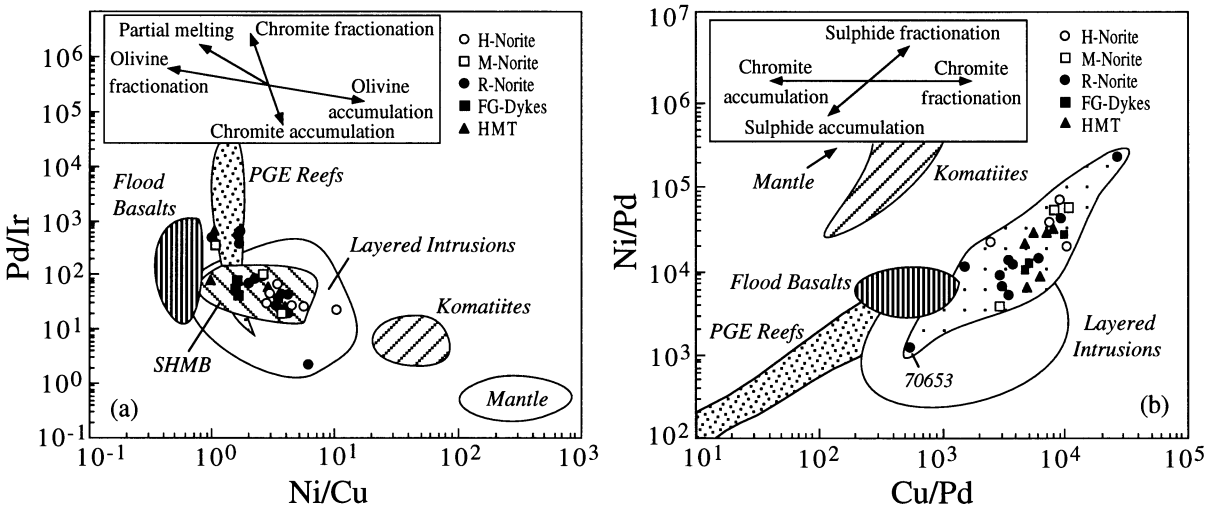

Fig. 7. Matel ratio diagrams of Pd/Ir vs Ni/Cu (a) and Ni/Pd vs Cu/Pd (b) showing the Vestfold Hills samples. Arrows indicate fractionation and accumulation trends. Compositional fields for PGE reefs, flood basalts, layered intrusions, SHMB, komatiites and mantle are taken from Naldrett (1981) and Barnes *et al.* (1988).

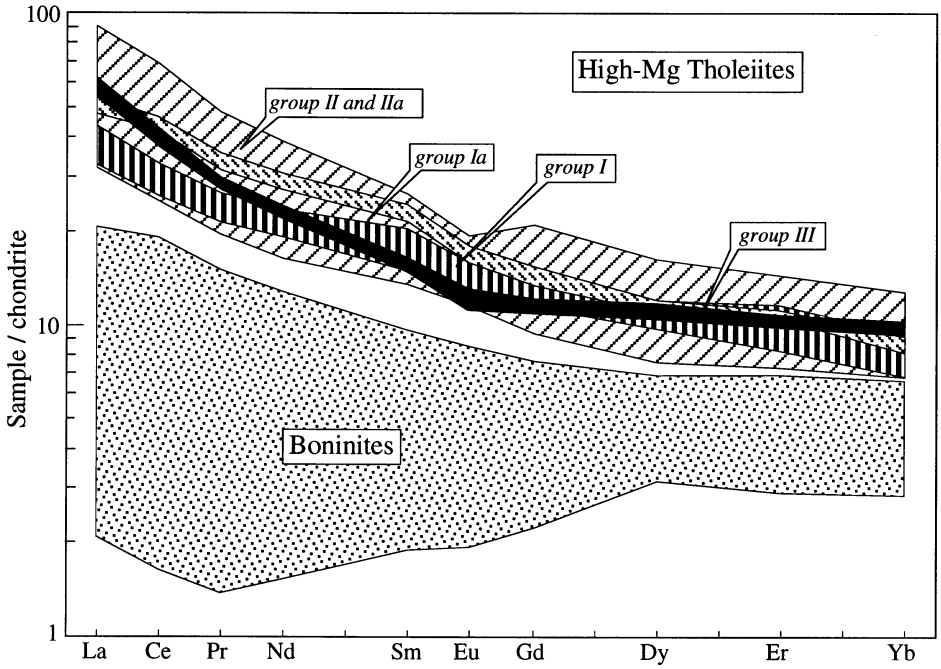

Fig. 8. Chondrite-normalized (Sun & McDonough, 1989) REE patterns from the Vestfold Hills HMT including the norites in comparison with boninites (Cameron *et al.*, 1983).

pyroxenite nodules requires a parental melt composition of *mg*-number ~76 using $K_D = 0{\cdot}3$ (Jaques & Green, 1979). This is at present the only evidence for the presence of a more primitive liquid. All other HMT dykes which have not experienced orthopyroxene accumulation are considerably more evolved, e.g. with *mg*-number <71 (Seitz, 1991).

Compositional variations in major and trace elements are consistent with differentiation controlled largely by orthopyroxene fractionation–accumulation and with an accumulation of orthopyroxene as well as Ni–Cu and Fe-sulphides for the Rubbly Norite (Seitz, 1991). It is suggested that Rubbly and Mottled Norite were derived from magmas which generated the Homogeneous Norite by the accumulation of up to 40% orthopyroxene, whereas the fine-grained dykes evolved from the Homogeneous Norite by the fractionation of ~20% orthopyroxene (Seitz, 1991).

There has been considerable debate over the petrogenesis of SHMB. Whereas Cameron *et al.* (1979) and Redman & Keays (1985) argued that the SHMB at Kambalda were Archaean analogues of boninites, Arndt & Jenner (1986) and Sun *et al.* (1989) concluded that they were crustally contaminated komatiites. Similarly, whereas Hamlyn & Keays (1986) and Hatton & Sharpe (1989) argued that the parental magmas to the Critical Zone of the Bushveld Complex were boninites, Sun *et al.* (1989) concluded that they were SHMB which had formed by crustal contamination of komatiites. It should be noted that neither Redman & Keays (1985) nor Hamlyn & Keays (1986) had the advantage of complete petrogenetic indicator element (LILE, HFSE, REE) data sets as did Sun *et al.* (1989). Further, Hatton & Sharpe (1989) argued against crustal contamination of the Bushveld Complex SHMB sills on the basis of physical considerations and not on geochemical grounds. In their paper, they showed that on geochemical grounds a boninitic magma could be derived from a komatiite by the addition of the appropriate gneissic rock. However, they disputed the hypothesis advanced by Huppert *et al.* (1984) that komatiite magmas had the ability to physically erode and assimilate large quantities of crustal material.

Although Kuehner (1989) suggested that SHMB in the Vestfold Hills might have been derived from boninitic magmas, he did so because of their similarity in composition to the Bushveld Complex SHMB, which Sharpe & Hulbert (1985) had concluded had been formed from boninitic magmas. Indeed, to avoid any petrogenetic implications, Kuehner (1989) used the term 'HMT' to describe the Vestfold Hills magmatic suite. Sheraton & Black (1981) found that there was no evidence of crustal contamination in the HMT dykes of the Vestfold Hills. On the other hand, Harley & Christy (1991, 1995) found crustal xenoliths in the Rubbly Norite, suggesting that crustal contamination may have played an important role.

Using a more complete petrogenetic indicator element suite than previous workers, Sun *et al.* (1989) argued that the Vestfold Hills SHMB had been formed from crustally contaminated komatiites.

The Homogeneous Norite as well as the HMT of the Vestfold Hills are characterized by high SiO_2 and MgO, and low TiO_2, features that are common to both SHMB and boninites. Sun *et al.* (1989) showed that the Vestfold Hills HMT have very similar petrogenetic indicator element patterns to Archaean SHMB volcanics as well as to the Bushveld Complex SHMB sills; in contrast, the patterns are different from those exhibited by boninites. Ranges for chondrite-normalized (Sun & McDonough, 1989) REE patterns are shown in Fig. 8 for boninites (Cameron *et al.*, 1983) and for HMT from the Vestfold Hills. Sun *et al.* (1989) noted that whereas boninites often have U-shaped REE patterns, SHMB have either flat or slightly sloping HREE patterns, or show continuous depletion from MREE to HREE. In addition, whereas boninitic magmas contain ~2% primary water, SHMB magmas are basically dry and contain only minor hydrous minerals. Also, at 10–12% MgO, boninites have 6–7% total FeO whereas SHMB have 10% total FeO. The low FeO contents of boninites indicate that they were derived from a refractory source. As seen in Table 7, boninites also have very low Ti and Y contents, also indicative of a strongly depleted source region. We concur with Sun *et al.* (1989) that the Vestfold Hills HMT are SHMB that are more likely to have formed from crustally contaminated komatiites rather than from boninitic magmas, which would have been derived from a strongly depleted source region.

DISCUSSION

The geochemical behaviour of the individual PGE is governed by their relative abilities to dissolve in silicate, metallic and sulphide phases (or their relative lithophile, siderophile and chalcophile character). The PGE are all strongly chalcophile with experimentally determined $D^{Pt,Pd}_{sulph-Sil}$ values of the order of 10^4 (Peach *et al.*, 1990, 1994). The PGE are thus preferentially partitioned into any sulphide phase which forms in an S-saturated basaltic magma. Accordingly, the S content and conditions leading to S saturation of basaltic magmas are critical to PGE behaviour. A magma's S-dissolving capacity is known to be a complex function of bulk composition, temperature, $f(O_2)$, $f(S_2)$ (Haughton *et al.*, 1974) and simple fractionation processes (Keays, 1995). A decrease in S solubility with differentiation may result in S saturation, precipitation and segregation of an immiscible sulphide liquid, which will efficiently scavenge PGE from the silicate magma.

During partial melting, the absence of a sulphide phase will result in relatively PGE-rich magmas (Keays, 1982, 1995; Hamlyn & Keays, 1986), whereas S saturation results in formation of a sulphide phase and a PGE-poor magma, owing to retention of the dense sulphide phase in the mantle source. Excellent examples of S-saturated magmas are mid-ocean ridge basalts (MORB), which are both PGE poor and S rich. Likewise, S saturation subsequent to melting will scavenge PGE and Cu from a magma into a separate sulphide melt phase, and may decouple the PGE from other metals which are not strongly chalcophile (e.g. Ni). In this way, the accumulation of sulphide melt droplets by gravity settling can produce PGE- and sulphide-rich cumulus horizons in magma chambers, such as the economically important PGE reefs in layered intrusions.

There are two mechanisms by which S-undersaturated magmas can be produced. The first mechanism involves high degrees of partial melting, which results in the production of magmas such as komatiites and picrites. Keays (1995) has shown that given an average of 250 p.p.m. S in undepleted upper mantle and an S capacity of 1000 p.p.m. in a partial melt, the minimum degree of partial melting required to produce an S-undersaturated melt is 25%. Given that komatiites are probably formed by at least 30% partial melting and possibly as much as 70% partial melting, they will be strongly S undersaturated. The second mechanism was suggested by Hamlyn & Keays (1986), who proposed that S-saturated melts produced by low to moderate degrees of partial melting of an undepleted mantle leave PGE-rich sulphides behind in the refractory upper residue. They termed such magmas 'first stage' partial melts and argued that, in addition to being S saturated, they would have very low PGE contents, which would remain with the residual immiscible sulphides. A good example of S-saturated first stage melts are MORBs, which contain average S concentrations of 800 p.p.m. (Moore & Fabbi, 1971), and low Pd concentrations (<0·83 p.p.b.: Crocket & Teruta, 1977; Hertogen *et al.*, 1980; Hamlyn & Keays, 1986), although higher concentrations have been reported (Crocket, 1981; Campbell *et al.*, 1983). On the other hand, second stage melts such as boninites, which are produced by partial melting of the refractory depleted mantle residue, are S undersaturated, low in TiO_2, and high in MgO and PGE, with abundances of <54 p.p.m. S and ~15 p.p.b. Pd (Hamlyn *et al.*, 1985).

Barnes *et al.* (1985) have detailed the specific effects of partial melting, crystal fractionation, sulphide saturation and other processes on the distribution of PGE and other metals (in particular, Ni and Cu) in basaltic magmas. In the absence of a sulphide phase, the PGE are sensitive to crystal fractionation and melting processes because the Iridium Group PGE (or IPGE; Ir, Os and Ru) and Ni are compatible in olivine, chromite and orthopyroxene (e.g. Agiorgitis & Wolf, 1978; Brügmann, 1985; Naldrett & Barnes, 1986; Brügmann *et al.*, 1987), whereas Cu and

Table 7: PGE, Au, Cu, Ti and Y abundances in variously derived mafic–ultramafic rocks

	MgO (%)	Pd (p.p.b.)	Ir (p.p.b.)	Pt (p.p.b.)	Au (p.p.b.)	Cu (p.p.m.)	Ti (p.p.m.)	Y (p.p.m.)	Ref.*
Fertile mantle	38	4	4	7	1	28	1300	4·6	1,3,4,6,9
Komatiites									
Abitibi, Canada	24	10	1·2	10	3	50	2400		
Eastern Goldfields	25	9	1·5	—	4·5	65	2300	10	5,12,13
Belingwe	18	12	0·5	12	(18)	73	2520	9	2,5,11
Gorgona Island	18	12	1·7	—	5	120	380	14	12
Picrites									
Disko Island	17·1	11	1·1	—	4	—	380	—	5
King Island		20	0·6	—	3	18	1600	—	5,7,8
SHMB									
Kambalda	10	16	0·35	—	5	95	3660	18	10
Mt Hunt	12	13	0·36	—	3	70	3480	16	10
Munni Munni	12	18	—	14	3	85	4000	11	13
Negri Volcanics	11	9	0·07	13	2	62	2460	14	13
Gooya Pooya	14	12	0·4	12	3	60	3000	12	13
Bushveld B4	12	12	0·35	17	3	56	2160	13	9
HMT									
Vestfold Hills	11	16	0·37	15	3	97	3960	13	14
Boninites									
Modern	12	17	<0·07	—	2	24	1200	6	7

*References: 1, Jagoutz *et al.* (1979); 2, Ross & Keays (1979); 3, Morgan *et al.* (1981); 4, Mitchell & Keays (1979); 5, Keays (1982); 6, Sun (1982); 7, Hamlyn *et al.* (1985); 8, Barnes *et al.* (1985); 9, Davies & Tredoux (1985); 10, Redman & Keays (1985); 11, Brügmann *et al.* (1987); 12, Barnes & Naldrett (1985); 13, Sun *et al.* (1991); 14, this study. —, not determined.

the Palladium Group PGE (or PPGE; Rh, Pt and Pd) are incompatible in these phases. Keays (1982) and Barnes *et al.* (1985) additionally suggested that the IPGE may form and fractionate as primary magmatic alloys from mafic magmas. Partial melting and crystal fractionation of basaltic magmas will thus produce relative enrichment of PPGE over IPGE. During crystallization of S-undersaturated ultramafic and mafic magmas, Pd (and the other PPGE) will behave incompatibly and become concentrated in the residual silicate melt (Ross & Keays, 1979; Naldrett & Barnes, 1986; Brügmann *et al.*, 1987; Keays, 1995). At the point of sulphide liquid unmixing, these elements become compatible and partition into the sulphide phase.

The low S contents (180 and 450 p.p.m.) of the chilled margins of the Vestfold Hills HMT dykes indicate that their parental magmas were very S undersaturated. This can be demonstrated using diagrams presented by Poulson & Ohmoto (1990), who confirmed data presented by Haughton *et al.* (1974), which showed that the solubility of S in a magma depends very strongly on its FeO content. Accordingly, at magmatic temperatures of ~1250°C the S capacity of the Vestfold Hills SHMB magmas, with FeO contents between 9·53 and 10·43 wt % (Table 2), would be about 1010 and 1230 p.p.m. S, respectively. Chilled margin sample 70533 has a composition of *mg*-number 68. However, the most primitive chilled margin composition observed in this dyke goes up to *mg*-number 71 (Seitz, 1991). The relative primitive composition of this dyke, which has not experienced orthopyroxene accumulation, may indicate, with its low S concentration (182 p.p.m.), that the parent magma was strongly S undersaturated. The higher S content of the more evolved samples is the result of differentiation processes (i.e. simple fractional crystallization), as S would accumulate in the residual magmas until S saturation was achieved. In addition, the high Pd and Pt contents of the chilled margins of the HMT dykes confirm that their parental magmas were S undersaturated, a fundamental requirement for the formation of major Cu–Ni–PGE sulphide deposits (Keays, 1995).

The strong depletion of IPGE relative to PPGE observed in all the HMT samples in Fig. 7a, is consistent with inter-element fractionation developed in response to preferential retention of the IPGE as Os–Ir alloys in the magma source regions or co-precipitation with early

fractionation ferromagnesian silicates and/or oxide phases during S-undersaturated conditions (see Mitchell & Keays, 1981; Keays, 1995). Given the primitive nature of most samples (*mg*-number ranging between 57 and 75; see Table 2) and their largely subparallel nature, the primary origin of PPGE–IPGE fractionation can be argued to arise through partial melting rather than crystal fraction processes.

The Vestfold Hills HMT have both high absolute PPGE abundances and high normalized PPGE relative to many other magma types (Fig. 6), the latter arising in part because of their high PPGE contents but also because of their low S abundances. Their chilled margins have almost identical absolute PGE abundances (average values: 16·0 p.p.b. Pd, 15·2 p.p.b. Pt, 0·98 p.p.b. Ru, 0·34 p.p.b. Ir) to SHMB volcanics and intrusives from Western Australia, as well as to the Bushveld Complex sills believed to represent the magmas that formed its Critical Zone (Table 7). In addition, their PPGE contents are very similar to those of boninites but considerably higher than those of komatiitic magmas (Table 7). Hamlyn *et al.* (1985) argued that boninites were derived from refractory upper mantle that had been depleted in S but enriched in the PGE that had been left behind in immiscible sulphides by first stage melts; the boninitic magmas would have inherited all of the PGE left behind by the first stage melts. If, on the other hand, SHMB are contaminated komatiites, as suggested by Sun *et al.* (1989), an explanation needs to be found for the higher Pd contents of SHMB relative to komatiites. This appears to lie in the model proposed by Sun *et al.* (1989), who argued that SHMB are products of AFC processes acting on komatiitic magmas in which the magmas undergo 35% crystal fractionation and ~14% assimilation of felsic crust. Given that komatiitic magmas contain ~10 p.p.b. Pd, 35% crystal fractionation would increase the Pd content of the residual melt to 13·5 p.p.b., assuming that no Pd was lost to the fractionating crystals. As the assimilated material would have also contained some Pd (perhaps 0·5 p.p.b.), it is clear that the Pd contents of SHMB could have been produced by AFC processes acting on komatiitic magmas.

Although SHMB, including those from the Vestfold Hills, have very similar Pd and Pt contents to boninites, they have markedly different Ir contents. With the exception of one Ir data point for the Negri Volcanics, all of the SHMB Ir data fall within a tight range, averaging 0·37 p.p.b. Ir (Table 7). On the other hand, 15 of the 28 samples that compose the modern boninite average of <0·07 p.p.b. Ir are reported as 'less than' figures by Hamlyn *et al.* (1985). Using an NiS fire assay preconcentration technique that had significantly lower detection limits than those of the technique used by Hamlyn *et al.* (1985), Peck & Keays (1990) obtained an average of 0·0705 and a range of 0·05–0·13 p.p.b. Ir for Cambrian boninites associated with the Heazlewood River Complex, Tasmania. It would appear, therefore, that another distinguishing feature of SHMB is that they have significantly higher Ir contents than boninites. In this connection, it is interesting that the Vestfold Hills HMT have identical Ir contents to other SHMB.

Although the parental magmas to the NRC were PGE bearing and S undersaturated, it is clear that they eventually became S saturated because the Rubbly Norite contains sulphide-rich zones which are also rich in the PGE. A model to explain this mineralization is proposed in the next section.

Model for sulphide mineralization

Given that the parental magmas to the NRC were S-undersaturated, PGE-bearing, SHMB magmas, we propose the following model to explain the origin of the Cu–Ni–PGE sulphide mineralization hosted by the Rubbly Norite. The komatiitic precursor to the SHMB magma would have been strongly S undersaturated (see Keays, 1995) before its assimilation of large quantities of crustal material and fractional crystallization, both of which would have pushed the SHMB magma so formed in the direction of S saturation, although the magma remained S undersaturated. The extensive fractionation of the magma would have led to a large increase in Pd and Pt contents but a decrease in Ir, Os and Ru (see Keays, 1995). The resultant SHMB magma was emplaced into the chamber occupied by the NRC, where it formed the Homogeneous Norite, Mottled Norite and fine-grained dykes with relatively low S contents. A part of the SHMB magma, however, was emplaced in a temporary chamber at a slightly deeper level than the NRC, in which it underwent cooling, fractionation (to generate orthopyroxene) and assimilation of some wall-rock material. Emplacement of the magma into this chamber caused cooling of the magma, as did assimilation of country rock material; both of these effects, as well as assimilation of SiO_2 and, possibly, S, from the country rocks led to a decrease in the S capacity of the magma. The crystallization of orthopyroxene, which settled to the floor of the temporary chamber, from the S-undersaturated magma caused an increase of S and, probably, Fe^{3+} in the residual melt. We suggest that these factors worked together to drive the magma towards S saturation and the generation of immiscible droplets of Cu–Ni–PGE sulphides, which accumulated along with the orthopyroxene phenocrysts that had settled towards the base of the temporary chamber. This phenocryst-laden and sulphide-bearing magma was then emplaced in the NRC magma chamber where it formed the Rubbly Norite.

Although SHMB magmas have been implicated in the formation of the Cu–Ni–PGE sulphide mineralization in

the major ore-bearing layered intrusions, this is the first example in which one can prove a direct link between SHMB magmas and Cu–Ni–PGE sulphide mineralization, albeit very small amounts. The reason why more magmatic sulphides are not present in the NRC is that SHMB magmas did not interact with an abundant S source, another fundamental requirement for the formation of major Cu–Ni–PGE sulphide mineralization (Keays, 1995).

ACKNOWLEDGEMENTS

This work was made possible through an ASAC grant held by Professor D. H. Green and logistic support of the Antarctic Division, Department of the Arts, Sports, Environment, Tourism and Territories. H.M.S. acknowledges receipt of a University of Tasmania scholarship. R.R.K. acknowledges receipt of ARC and AINSE grants. D. H. Green, Steve Eggins and Russell Sweeney are thanked for helpful discussions and reviewing an earlier version of this manuscript. Simon Harley (editorial handling), Beate Orberger and an anonymous reviewer provided very useful comments on the manuscript.

REFERENCES

Agiorgitis, G. & Wolf, R., 1978. Aspects of osmium, ruthenium and iridium contents in some Greek chromites. *Chemical Geology* **23,** 267–272.

Arndt, N. T. & Jenner, G. A., 1986. Crustally contaminated komatiites and basalts from Kambalda, Western Australia. *Chemical Geology* **56,** 229–255.

Barnes, S. J. & Naldrett, A. J., 1985. Geochemistry of the J-M reef of the Stillwater Complex, Minneapolis Adit Area. I Sulfide chemistry and sulfide–olivine equilibrium. *Economic Geology* **80,** 627–645.

Barnes, S.-J., Naldrett, A. J. & Gorton, M.P., 1985. The origin of the fractionation of platinum-group elements in terrestrial magmas. *Chemical Geology* **53,** 303–323.

Barnes, S. J., Boyd, R., Korneliussen, A., Nilsson, L. P., Often, M., Pederson, R. B. & Robins, B., 1988. The use of mantle normalized and metal ratios in discriminating between the effects of partial melting, crystal fractionation and sulphide segregation on platinum-group elements, gold, nickel and copper: examples from Norway. In: Pichard, H. M., Potts, P. J., Barles, J. F. W. & Cribb, S. J. (eds) *Geo-Platinum*. Barking, UK: Elsevier Applied Science, pp. 113–143.

Black, L. P., Kinny, P. D. & Sheraton, J. W., 1991. The difficulties of dating mafic dykes: an Antarctic example. *Contributions to Mineralogy and Petrology* **109,** 183–194.

Brügmann, G. E., 1985. Geochemistry of noble metals and lithophile elements in komatiite flows from Alexo, Canada and Gorgona, Colombia. Ph.D. Thesis, Johannes Gutenberg-Universität, Mainz, 261 pp.

Brügmann, G. E., Arndt, N. T., Hofmann, A. W. & Tobschall, H. J., 1987. Noble metal abundances in komatiite suite from Alexo, Ontario, and Gorgona Island, Colombia. *Geochimica et Cosmochimica Acta* **51,** 2159–2169.

Campbell, I. H., Naldrett, A. J. & Barnes, S. J., 1983. A model for the origin of the platinum-rich sulfide horizons in the Bushveld and Stillwater Complexes. *Journal of Petrology* **24,** 133–165.

Cameron, W. E., Nisbet, E. G. & Dietrich, V. J., 1979. Boninite, komatiites and ophiolitic basalts. *Nature* **280,** 550–553.

Cameron, W. E., McCulloch, M. T. & Walker, D. A., 1983. Boninite petrogenesis: chemical and Nd–Sr isotopic constraints. *Earth and Planetary Science Letters* **65,** 75–89.

Collerson, K. D. & Sheraton, J. W., 1986. Bedrock geology and crustal evolution of the Vestfold Hills. In: Pickard, J. (ed.) *The Antarctic Oasis: Terrestrial Environments and History of the Vestfold Hills*. Sydney: Academic Press, pp. 21–62.

Collerson, K. D., Sheraton, J. W. & Arriens, P. A., 1983. Granulite facies metamorphic conditions during the Archaean evolution and late Proterozoic reworking of the Vestfold Block, Eastern Antarctica. *Sixth Australian Geological Convention, Canberra, Abstracts*, pp. 53–54.

Crocket, J. H., 1981. Geochemistry of the platinum group elements. In: Cabri, L. J. (ed.) *Platinum Group Elements. Mineralogy, Geology and Exploration. Canadian Institute of Mining and Metallurgy Special Volume* 47–64.

Crocket, J. H. & Teruta, Y., 1977. Palladium, iridium and gold contents of mafic and ultramafic rocks drilled from the Mid-Atlantic Ridge, Leg 37, Deep Sea Drilling Project. *Canadian Journal of Earth Sciences* **14,** 777–784.

Davies, G. & Tredoux, M., 1985. The platinum-group element and gold contents of marginal rocks and sills of the Bushveld Complex. *Economic Geology* **80,** 838–848.

Dirks, P. H. G. M., Hoek, J. D., Wilson, C. J. L. & Sims, J. R., 1994. The Proterozoic deformation of the Vestfold Hills Basement complex, East Antarctica; implications for the tectonic development of adjacent granulite belts. *Precambrian Research* **65,** 277–295.

Green, D. H., 1970. The origin of basaltic and nephelinitic magmas. *Leicester Literary and Philosophical Society Transactions* **64,** 28–54.

Green, D. H., 1971. Composition of basaltic magmas as indicators of conditions of origin: application to oceanic volcanism. *Philosophical Transactions of the Royal Society of London* **268,** 707–725.

Hamlyn, P. R. & Keays, R. R., 1986. Sulfur saturation and second stage melts: applications to the Bushveld platinum metal deposits. *Economic Geology* **81,** 1431–1445.

Hamlyn, P. R., Keays, R. R., Cameron, W. E., Crawford, A. J. & Waldron, H. M., 1985. Precious metals in magnesian low-Ti lavas: implications for metallogenesis and sulphur saturation in primary magmas. *Geochimica et Cosmochimica Acta* **49**, 1797–1811.

Harley, S. L. & Christy, A. G., 1991. Titanian 2:2:1 sapphirine in Mg–Al rich gneiss xenoliths from the Northern Vestfold Hills: a first record and implications for emplacement pressures of the Long Peninsula Norite Complex. *6th International Symposium on Antarctic Earth Sciences, Abstracts*. Ranzan-Machi, Japan: National Institute of Polar Research, pp. 211–212.

Harley, S. L. & Christy, A. G., 1995. Titanium-bearing sapphirine in a partially melted aluminous granulite xenolith, Vestfold Hills, Antarctica. *European Journal of Mineralogy* **7,** 637–653.

Hatton, C. J. & Sharpe, M. R., 1989. Significance and origin of boninite-like rocks associated with the Bushveld Complex. In: Crawford, A. J. (ed.) *Boninites and Related Rocks*. London: Unwin Hyman, pp. 174–207.

Haughton, D. R., Roeder, P. L. & Skinner, B. J., 1974. Solubility of sulphur in mafic magmas. *Economic Geology* **69,** 457–467.

Hertogen, J., Janssen, M. J. & Palme, H., 1980. Trace elements in ocean ridge basalt glasses: implications for fractionation during mantle evolution and petrogenesis. *Geochimica et Cosmochimica Acta* **44,** 2125–2143.

Hoatson, D. M. & Keays, R. R., 1989. Formation of platiniferous sulfide horizons by crystal fractionation and magmatic mixing in the Munni Munni layered intrusion, West Pilbara Block, Western Australia. *Economic Geology* **84,** 1775–1804.

Hoek, J. D. & Passchier, C. W., 1991. The Proterozoic structural evolution of the Vestfold Hills, an Archaean craton in a Proterozoic metamorphic belt, East Antarctic Shield. *6th International Symposium on Antarctic Earth Sciences, Abstracts*. Ranzan-Machi, Japan: National Institute of Polar Research, 231 pp.

Hoek, J. D. & Seitz, H.-M., 1995. Continental mafic dyke swarms as tectonic indicators: an example from the Vestfold Hills, East Antarctica. *Precambrian Research* **75,** 121–139.

Huppert, H. E., Sparks, R. S. J., Turner, J. S. & Arndt, N. T., 1984. Emplacement and cooling of komatiite lavas. *Nature* **309,** 19–22.

Jagoutz, E., Palme, H., Baddenhausen, H., Blum, K., Cendales, M., Dreibus, G., Spettel, B., Lorenz, V. & Wänke, H., 1979. The abundances of major, minor and trace elements in the earth's mantle as derived from primitive ultramafic nodules. *Proceedings, 10th Lunar and Planetary Science Conference. Geochimica et Cosmochimica Acta Supplement* 2031–2050.

James, P. R. & Tingey, R. J., 1983. The Precambrian geological evolution of the East Antarctic metamorphic shield—a review. In: Oliver, R. L., James, P. R. & Jago, J. B. (eds) *Antarctic Earth Science*. Canberra, A.C.T.: Australian Academy of Sciences, pp. 5–10.

Jaques, A. L. & Green, D. H., 1979. Determination of liquid compositions in high-pressure melting of peridotite. *American Mineralogist* **64,** 1312–1321.

Keays, R. R., 1982. Palladium and iridium in komatiites and associated rocks, application to petrogenetic problems. In: Arndt, N. T. & Nisbet, E. G. (eds) *Komatiites*. London: Allen, pp. 435–438.

Keays, R. R., 1983. Archaean gold deposits and their source rocks: the upper mantle connection. In: Foster, R. P. (ed.) *Gold '82—the Geology, Geochemistry and Genesis of Gold Deposits*. Rotterdam: A. A. Balkema, pp. 17–51.

Keays, R. R., 1987. Principles of mobilization (dissolution) of metals in mafic and ultramafic rocks: the role of immiscible magmatic sulphides in the generation of hydrothermal gold and volcanogenic massive sulphide deposits. *Ore Geology Reviews* **2,** 47–63.

Keays, R. R., 1995. The role of komatiitic and picritic magmatism and S-saturation in the formation of ore deposits. *Lithos* **34,** 1–18.

Klemm, D. D., 1965. Synthesen und Analysen in den Dreiecksdiagrammmen Fe As S–Co As S–Ni As S und FeS_2–CoS_2–NiS_2. *Neues Jahrbuch für Mineralogie, Abhandlungen* **103**(3), 205–255.

Kuehner, S. M., 1986. Mafic dykes in the East Antarctic shield: experimental, geochemical and petrological studies focusing on the Proterozoic evolution of the crust and mantle. Ph.D. Thesis, University of Tasmania, Hobart.

Kuehner, S. M., 1987. Mafic dykes of the East Antarctic Shield: a note on the Vestfold Hills and Mawson Coast occurrences. In: Hall, H. C. & Fahrig, W. F. (eds) *Mafic Dyke Swarms. Geological Association of Canada, Special Paper* **34,** 429–430.

Kuehner, S. M., 1989. Petrology and geochemistry of early Proterozoic high-Mg dykes from the Vestfold Hills, Antarctica. In: Crawford, A. R. (ed.) *Boninites and Related Rocks*. London: Unwin Hyman, pp. 208–231.

Kuehner, S. M. & Green, D. H., 1987. Uplift history of the East Antarctic shield: constraints imposed by high-pressure experimental studies of Proterozoic mafic dykes. In: Thomson, M. R. A., Crame, J. A. & Thomson, J. W. (eds) *Geological Evolution of Antarctica. Proceedings of the 5th International Symposium of Antarctic Earth Sciences*. Cambridge: Cambridge University Press, pp. 1–6.

Lanyon, R., Black, L. P. & Seitz, H.-M., 1993. U–Pb zircon dating of mafic dykes and its application to the Proterozoic geological history of the Vestfold Hills, East Antarctica. *Contributions to Mineralogy and Petrology* **115,** 184–203.

McLeod, J. R. & Harding, R. R., 1967. Age of dolerite dykes in the Vestfold Hills, Antarctica. *Nature* **215,** 149–151.

Mitchell, R. H. & Keays, R. R., 1979. Palladium, gold and iridium in mantle minerals. Implications for models of magma genesis. *Abstract IUGG Meeting*. Canberra: International Union of Geodesy and Geophysics, p. 259.

Mitchell, R. H. & Keays, R. R., 1981. Abundance and distribution of gold, palladium and iridium in some spinel and garnet lherzolites: implications for the nature and origin of precious metal-rich intergranular components in the upper mantle. *Geochimica et Cosmochimica Acta* **45,** 5425–5442.

Moore, J. G. & Fabbi, B., 1971. An estimate of the juvenile sulfur content of basalts. *Contributions to Mineralogy and Petrology* **33,** 118–127.

Morgan, J. W., Wandless, G. A., Petrie, R. K. & Irving, A. J., 1981. Composition of earth's upper mantle—I. Siderophile trace elements in ultramafic nodules. *Tectonophysics* **75,** 47–67.

Naldrett, A. J., 1981. Platinum-group element deposits. *Canadian Institute of Mining and Metallurgy, Special Issue* **23,** 197–232.

Naldrett, A. J. & Barnes, S. J., 1986. The fractionation of platinum-group elements with special reference to the composition of sulphide ores. *Fortschritte der Mineralogie* **64,** 113–133.

Naldrett, A. J. & Duke, J. M., 1980. Pt metals in magmatic sulfide ores; the occurrence of these metals is discussed in relation to the formation and importance of these ores. *Science* **208,** 1417–1424.

Naldrett, A. J., Hoffmann, E. L., Green, A. H., Chou, C. L. & Naldrett, S. R., 1979. The composition of Ni-sulfide ores with particular reference to their content of PGE and Au. *Canadian Mineralogist* **17,** 403–415.

Oliver, R. L., James, P. R., Collerson, K. D. & Ryan, A. B., 1982. Precambrian geological relationships in the Vestfold Hills, Antarctica. In: Craddock, C. (ed.) *Antarctic Geoscience*. Madison, WI: University of Wisconsin Press, pp. 435–444.

Palme, H., Baddenhausen, H., Blum, K., Cendales, M., Dreibus, G., Hofmeister, H., Palme, C., Spettel, B., Vilcsek, E. & Wanke, H., 1978. New data on lunar samples and achondrites and a comparison of the least fractionated samples from the Earth, the Moon and the eucrite parent body. *Proceedings, 9th Lunar and Planetary Science Conference. Geochimica et Cosmochimica Acta Supplement* 25–57.

Parker, A. J., James, P. R., Mielnik, V. & Oliver, R. L., 1983. Structure, fabric development and metamorphism in Archaean gneisses of the Vestfold Hills, East Antarctica. In: Oliver, R. L., James, P. R. & Jago, J. B. (eds) *Antarctic Earth Science*. Canberra, A.C.T.: Australian Academy of Sciences, pp. 85–90.

Passchier, C. W., Hoek, J. D., Bekendam, R. F. & de Boorder, H., 1990. Ductile reactivation of Proterozoic brittle fault rocks; an example from the Vestfold Hills, East Antarctica. *Precambrian Research* **47,** 3–16.

Peach, C. L., Mathez, E. A. & Keays, R. R., 1990. Sulfide melt–silicate melt distribution coefficients for noble metals and other chalcophile elements as deduced from MORB: implications for partial melting. *Geochimica et Cosmochimica Acta* **54,** 3379–3389.

Peach, C., Mathez, E. A., Keays, R. R. & Reeves, S. J., 1994. Experimentally determined sulfide melt–silicate melt partition coefficients for iridium and palladium. *Chemical Geology* **117,** 361–377.

Peck, D. C. & Keays, R. R., 1990. Geology, geochemistry and origin of platinum group element–chromitite occurrences in the Hazelwood River Complex, Tasmania. *Economic Geology* **85,** 765–793.

Poulson, S. R. & Ohmoto, H., 1990. An evaluation of the solubility of sulfide sulfur in silicate melts from experimental data and natural samples. *Chemical Geology* **85,** 57–75.

Redman, B. A. & Keays, R. R., 1985. Archaean basic volcanism in the Eastern Goldfields Province, Yilgarn Block, Western Australia. *Precambrian Research* **30,** 113–152.

Robinson, P., Higgins, N. C. & Jenner, G. A., 1986. Determination of rare-earth elements, yttrium and scandium rocks by an ion exchange–X-ray fluorescence technique. *Chemical Geology* **55,** 121–137.

Ross, J. R. & Keays, R. R., 1979. Precious metals in volcanic-type nickel sulfide deposits in Western Australia, 1. Relationships with the composition of the ores and host rocks. *Canadian Mineralogist* **1,** 417–436.

Seitz, H.-M., 1991. Geochemistry and petrogenesis of high-Mg tholeiites and lamprophyres in the Vestfold Hills, Antarctica. Ph.D. Thesis, University of Tasmania, Hobart.

Seitz, H.-M., 1994. Estimation of emplacement pressure for 2350 Ma high-Mg tholeiite dykes, Vestfold Hills, Antarctica. *European Journal of Mineralogy* **6,** 195–208.

Sharpe, M. R. & Hulbert, L. J., 1985. Ultramafic sills beneath the Eastern Bushveld Complex: mobilized suspensions of early lower zone cumulates in a parental magma with boninitic affinities. *Economic Geology* **80,** 849–871.

Sheraton, J. W. & Black, L. P., 1981. Geochemistry and geochronology of Proterozoic tholeiite dykes of East Antarctica: evidence for mantle metasomatism. *Contributions to Mineralogy and Petrology* **78,** 305–317.

Sheraton, J. W. & Collerson, K. D., 1983. Archaean and Proterozoic geological relationships in the Vestfold Hills–Prydz Bay area, Antarctica. *Bureau of Mineral Resources Journal of Australian Geology and Geophysics* **8,** 119–128.

Sun, S.-S., 1982. Chemical composition and origin of the Earth's primitive mantle. *Geochimica et Cosmochimica Acta* **46,** 179–192.

Sun, S.-S. & McDonough, W. F., 1989. Chemical and isotopic systematics of oceanic basalts: implications for mantle composition and processes. In: Sanders, A. D. & Norry, M. J. (eds) *Magmatism in Ocean Basins. Geological Society of London, Special Publication* **42,** 315–345.

Sun, S.-S., Wallace, D. A., Hoatson, D. M., Glikson, A. K. & Keays, R. R., 1991. Use of geochemistry as a guide to platinum group element potential of mafic–ultramafic rocks: examples from the West Pilbara and Halls Creek Mobile Zone, Western Australia. *Precambrian Research* **50,** 1–35.

Wager, L. R., Brown, G. M. & Wadsworth, W. I., 1960. Types of igneous cumulates. *Journal of Petrology* **1**(1), 73–85.